

Black holes from large N singlet models

Irene Amado¹, Bo Sundborg¹, Larus Thorlacius^{1,2} and Nico Wintergerst^{1,3}

¹*The Oskar Klein Centre for Cosmoparticle Physics, Department of Physics, Stockholm University, AlbaNova, 106 91 Stockholm, Sweden*

²*University of Iceland, Science Institute, Dunhaga 3, 107 Reykjavik, Iceland*

³*The Niels Bohr Institute, University of Copenhagen, Blegdamsvej 17, 2100 Copenhagen Ø, Denmark*

E-mail: irene.amado@fysik.su.se, bo@fysik.su.se,
larus.thorlacius@fysik.su.se, nico.wintergerst@nbi.ku.dk

ABSTRACT: The emergent nature of spacetime geometry and black holes can be directly probed in simple holographic duals of higher spin gravity and tensionless string theory. To this end, we study time dependent thermal correlation functions of gauge invariant observables in suitably chosen free large N gauge theories. At low temperature and on short time scales the correlation functions encode propagation through an approximate AdS spacetime while interesting departures emerge at high temperature and on longer time scales. This includes the existence of evanescent modes and the exponential decay of time dependent boundary correlations, both of which are well known indicators of bulk black holes in AdS/CFT. In addition, a new time scale emerges after which the correlation functions return to a bulk thermal AdS form up to an overall temperature dependent normalization. A corresponding length scale was seen in equal time correlation functions in the same models in our earlier work.

Contents

1	Introduction	2
2	Eigenvalue distributions and large-N phase transitions	4
2.1	Vector model	5
2.2	Adjoint model	6
3	Time dependent correlators	7
4	Evanescent modes	9
5	General behavior of two-point correlation functions	12
5.1	Coincident points	12
5.2	Low temperatures: Power laws	14
5.3	Ultra-high temperatures	14
5.3.1	Even dimensions: Exponential decay	15
5.3.2	Odd dimensions: Retarded Green's functions supported inside the light cone	16
5.4	Intermediate temperatures: Numerical results	17
6	Finite volume effects in the high temperature phase	20
7	Discussion	24
A	Saddle point evaluation of path integrals and eigenvalue distributions	27
B	Time dependent Green functions	30
C	Fourier space	33
C.1	Retarded propagator	33
C.2	Evanescence	33
D	Consistency check on bulk and boundary retarded propagator support	34

1 Introduction

The singlet sector of large N gauge theories coupled to vector or adjoint representation scalar matter provides a tractable framework for studying gauge/gravity duality in an interesting limit where the 't Hooft coupling vanishes. In this limit various explicit computations can be carried out on the gauge theory side and it is an interesting question to what extent the results may be interpreted in terms of an emergent bulk spacetime on the gravity side. We consider two classes of singlet models in various dimensions, with matter fields in the vector or adjoint representation of the gauge group. A representative of each class can be obtained as the free limit of an interacting gauge theory arising in well-studied examples of gauge/gravity duality. Three dimensional Chern-Simons large N gauge theory with matter fields in the vector representation of the gauge group is conjectured to be dual [1–3] to Vasiliev higher spin theory [4, 5] while four dimensional Yang-Mills theory with adjoint matter fields is dual to strings in an AdS background. The latter is of course the standard AdS/CFT duality but in the limit of zero 't Hooft coupling the strings on the gravity side are tensionless and the dynamics includes an infinite tower of higher spin states in addition to the usual massless sector involving the graviton and dilaton [6].

A key aspect of gauge/gravity duality is the connection between thermal states in the field theory and black holes in the bulk [7]. Due to the singlet constraint, the free gauge theories considered here exhibit non-trivial thermal behavior, including large N phase transitions at finite volume, even in the limit of vanishing coupling [8]. In recent work [9], we have extended the thermodynamic analysis of these models by considering equal time correlation functions at thermal equilibrium in the boundary theory and analyzing their spatial structure as a function of temperature. At low temperature our results are consistent with propagation through an AdS bulk geometry with non-trivial additional structure appearing above the phase transition. This holds for both adjoint and vector matter, but the geometric features that arise at high temperature do so on very different length scales in the two types of models. For adjoint matter the phase transition is at the AdS scale and a good case can be made for the black hole interpretation by turning on interactions and going to strong coupling where the large N phase transition is transmuted into the Hawking-Page transition and the high temperature phase is dominated by bulk black holes [7]. For vector matter, on the other hand, the phase transition temperature in the free theory grows with a power of N compared to the AdS scale in the large N limit [10] and any dual bulk objects would appear at a characteristic length scale that is much larger than the AdS length [9].

In classical gravity a black hole can be detected by its effect on the time evolution of matter in its environment, for instance in-falling particles or waves. Boundary correlation functions encode such information in their time dependence. In the present paper we therefore extend our previous work to the temporal sector of the singlet models and gather more direct evidence for black hole-like behavior in the emergent dual bulk spacetime. We map out characteristic features of temporal correlations at different temperatures and compare them to known black hole signatures in strongly coupled field theories. The overall structure is

similar in theories with vector and adjoint matter but there are important differences and we point these out as we go along. We note that a closely related problem has been studied earlier in planar AdS/CFT with the standard $\mathcal{N} = 4$ SYM theory on the boundary [11]. Having a spherical boundary is essential for our work as it permits us to resolve thermal phase transitions and study their influence on correlation functions. We can compare our results to the planar case by taking the limit of ultra-high temperatures and considering short distances and times relative to the size of the spatial sphere.

We find it useful to consider free singlet theories in general dimensions as toy models but it is only for the canonical values of three and four dimensions, for theories with vector and adjoint matter respectively, that one expects to find interacting conformal theories when the gauge coupling is turned on. By keeping the dimension general, we observe qualitatively different time dependence of the boundary correlation functions between even and odd boundary dimensions. This is related to well-known differences in wave propagation in even and odd dimensions but seems to have received limited attention in the AdS/CFT literature where the main focus has been on spatial correlations and on even boundary dimensions.

Our main results may be listed as follows:

1. At high temperature, the imaginary part of the Fourier space retarded propagator receives exponentially suppressed, but non-vanishing, contributions at $k \gg T \gg \omega$. This shows the presence of so called evanescent modes which are characteristic of an event horizon in a bulk black hole spacetime.
2. Boundary correlation functions depart significantly from thermal AdS boundary-to-boundary Green's functions at high temperature, as should be the case in the presence of a localized central object in the bulk.
 - (a) In even boundary dimensions, they undergo a period of rapid exponential decay, as is known to occur in an AdS black hole background in Einstein gravity.
 - (b) In odd boundary dimensions, the retarded Green's function develops support inside the light cone.
3. For low boundary dimensions, high-temperature correlators exhibit a characteristic time scale beyond which their form returns to that of thermal AdS correlators with a temperature dependent normalization factor. This feature, suggesting further localized structure, is also seen in higher boundary dimensions, but then only over a finite range of temperatures above the critical temperature.

The paper is planned along the following lines. Section 2 contains some background on the models under study and their large N phase transitions. This is well known material that we include to establish notation and set the stage for what follows. In Section 3 we express the time dependent correlation function of a pair of singlet operators at finite temperature in terms of the distribution of eigenvalue of the $U(N)$ gauge holonomy around the thermal S^1 .

The resulting formulas are analyzed in the remainder of the paper. We first focus on properties of the retarded propagator in Section 4 and find that evanescent modes (item 1 above) are present in the high-temperature phase with adjoint matter, while for vector matter they are already discernible below the phase transition at temperatures that are parametrically comparable to the critical temperature. The existence of such modes has been argued previously from a collective field theory approach to thermo-field dynamics of the boundary theory in a high-temperature limit, well above the phase transition [12, 13]. Our results provide a direct confirmation of evanescent modes in singlet models at any temperature that is sufficiently high for the eigenvalue distribution to deviate from a flat distribution. In Section 5 we turn to a comprehensive analysis of the time-ordered correlator, mainly using analytic methods but also presenting results obtained by numerical means. We establish a period of exponential decay in time of correlations in even boundary dimensions and show that the retarded Green’s function is non-zero in the interior of the light cone in odd dimensions (as per item 2 above). For intermediate temperatures, a detailed numerical study is presented in Section 5.4. In particular, we point out features that a naive high-temperature expansion fails to capture. Those features are then the focus of Section 6, where we catch a glimpse of intriguing finite volume behavior in the high temperature phase (item 3). Beyond a certain timescale, the boundary correlation functions return to the form of thermal boundary-to-boundary propagators in an AdS bulk geometry, dressed by a temperature dependent normalization factor. We wrap up with a discussion in Section 7 and this is followed by several appendices with additional technical details and background material.

2 Eigenvalue distributions and large- N phase transitions

One of our main goals is to calculate time dependent correlation functions in $U(N)$ gauge theories in the limit of vanishing gauge coupling with a view towards an interpretation in terms of emergent spacetime geometry in a dual gravitational theory. We consider matter in the form of a free scalar field in the adjoint representation of the gauge group or a finite number N_f of scalars in the fundamental representation. We work at finite volume and finite temperature with fields defined on a spatial unit $d-1$ -sphere and a thermal circle $t \cong t + i\beta$.

In free gauge theories, extracting nontrivial thermodynamic features is a matter of counting singlet operators, for example by Polya’s method, as done in the original work [8], where the projection to singlets was also introduced by hand as a matrix model for a $U(N)$ valued Lagrange multiplier. Alternatively, one can derive the matrix integral from the path integral expression for the partition function [14] for interacting gauge theory. By viewing the singlet constraint as the residual Gauss law of the gauge theory at zero coupling, the Lagrange multiplier has a straightforward interpretation as the $U(N)$ gauge holonomy around the thermal circle.

At large N , the matrix model can be solved in a saddle point approximation. This is achieved by approximating the integral over the eigenvalues of the matrix valued Lagrange multiplier as a path integral over an eigenvalue distribution $\rho(\lambda)$. Extremizing the corre-

sponding action leads to a saddle point expression for $\rho(\lambda)$, which in turn governs the physical behavior of correlation functions. Derivations of $\rho(\lambda)$ for matter in the adjoint and fundamental representations can be found in [8, 10, 14, 15] and we summarize the main steps involved in Appendix A.

2.1 Vector model

The saddle point value of the eigenvalue density in a theory with N_f scalar fields in the fundamental representation of $U(N)$ is [15]

$$\rho(\lambda) = \frac{1}{2\pi} + \frac{N_f}{N} \sum_{k=1}^{\infty} z_S^d(x^k) \frac{1}{\pi} \cos(k\lambda), \quad (2.1)$$

where $-\pi \leq \lambda \leq \pi$ and $z_S^d(x)$ is the one-particle partition sum on a $d-1$ -dimensional sphere,

$$z_S^d(x) = x^{\frac{d}{2}-1} \frac{1+x}{(1-x)^{d-1}}, \quad (2.2)$$

with $x = e^{-\beta}$. Here, and in the following, we have chosen units in which the sphere has unit radius and $\beta = 1/T$ is dimensionless.

The eigenvalue density is constrained to be positive and satisfies the normalization condition $\int d\lambda \rho(\lambda) = 1$. Low temperature corresponds to $x \ll 1$ and it immediately follows from (2.1) that the eigenvalue distribution is flat,

$$\rho(\lambda) \approx \frac{1}{2\pi}, \quad (2.3)$$

in the limit of low temperature and large N . At high temperature, on the other hand, we have $x \rightarrow 1$. In this case the one-particle partition sum simplifies and the eigenvalue density reduces to

$$\rho(\lambda) = \frac{1}{2\pi} + \frac{2N_f}{\pi N} T^{d-1} \sum_{k=1}^{\infty} \frac{\cos(k\lambda)}{k^{d-1}}. \quad (2.4)$$

This expression is valid as long as $\rho(\lambda)$ remains everywhere positive but this fails at a critical temperature,

$$T_c^{d-1} = \frac{1}{4(1-2^{2-d})\zeta(d-1)} \frac{N}{N_f}, \quad (2.5)$$

at which $\rho(\pm\pi) \rightarrow 0$. The critical temperature T_c , which is parametrically high in this model, signals a third order phase transition [15].

The shape of the eigenvalue distribution at different temperatures is shown in Fig. 1. Above the phase transition the eigenvalue density vanishes beyond a certain maximal value λ_m determined by the normalization condition $\int_{-\lambda_m}^{\lambda_m} \rho(\lambda) d\lambda = 1$. Explicit formulas are given in Appendix A for the eigenvalue density at high temperature as well as for the maximal eigenvalue λ_m above the phase transition. At very high temperatures the eigenvalue density becomes narrowly peaked around the origin and approaches a Dirac delta function in the

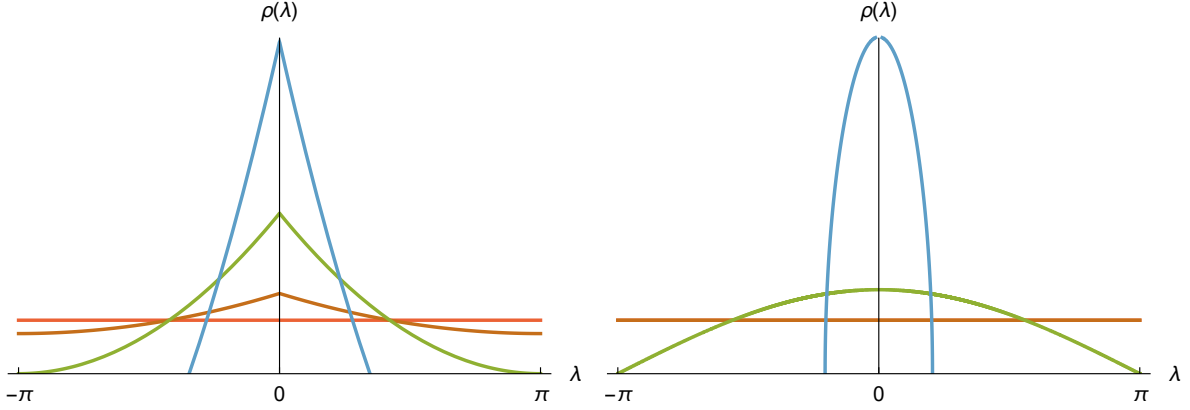


Figure 1. *Left:* Eigenvalue distribution in vector model at $d = 3$ for $T/T_c \ll 1$ (red), $T/T_c = 1/2$ (orange), $T/T_c = 1$ (green) and $T/T_c \approx 2$ (blue). *Right:* Eigenvalue distribution in adjoint model at $d = 4$ for $T/T_c \ll 1$ (red), $T/T_c = 1/2$ (orange), $T/T_c = 1$ (green) and $T/T_c \approx 2$ (blue). In this case, curve remains the same for all $T \leq T_c$ and the phase transition is first order. For $T/T_c \rightarrow \infty$, the distribution approaches a δ -function in both models.

$T \rightarrow \infty$ limit. For later reference, we here quote the scaling formulas for the width of the distribution at high temperature, $T \gg T_c$, in different spatial dimensions, as derived in Appendix A,

$$\lambda_m \rightarrow \frac{T_c}{T} \times \begin{cases} \sqrt{\frac{2}{\pi A_d}} & \text{for } d = 3, \\ \left(\frac{3}{2A_d}\right)^{\frac{1}{3}} \log^{-1/3} \frac{T}{T_c} & \text{for } d = 4, \\ \left(\frac{3}{2\zeta(d-3)A_d}\right)^{\frac{1}{3}} \left(\frac{T_c}{T}\right)^{\frac{d-4}{3}} & \text{for } d \geq 5. \end{cases} \quad (2.6)$$

In particular, $\lambda_m \sim T_c/T$ in $d = 3$, the canonical dimension for the vector model.

2.2 Adjoint model

The thermodynamic behavior is similar when the matter field is in the adjoint representation of the gauge group but there are important differences. In particular, the critical temperature remains finite in the large N limit and the phase transition is first order. The eigenvalue distribution is shown in the right hand panel in Figure 1. It remains flat, $\rho(\lambda) = \frac{1}{2\pi}$, at all temperatures below the phase transition but above the transition the eigenvalue density develops a non-trivial profile that can be approximated by the following expression [14],

$$\rho(\lambda) = \begin{cases} \frac{1}{\pi \sin^2(\frac{\lambda_m}{2})} \sqrt{\sin^2(\frac{\lambda_m}{2}) - \sin^2(\frac{\lambda}{2})} \cos(\frac{\lambda}{2}) & \text{if } 0 \leq |\lambda| \leq \lambda_m, \\ 0 & \text{if } \lambda_m < |\lambda| \leq \pi. \end{cases} \quad (2.7)$$

The maximal eigenvalue λ_m is determined by

$$\sin^2\left(\frac{\lambda_m}{2}\right) = 1 - \sqrt{1 - \frac{1}{z_S^d(x)}}. \quad (2.8)$$

At high temperature, $T \gg T_c$, the eigenvalue distribution of the adjoint model becomes narrowly peaked,

$$\rho(\lambda) \approx \frac{2}{\pi \lambda_m} \sqrt{1 - \frac{\lambda^2}{\lambda_m^2}}, \quad (2.9)$$

with the maximal eigenvalue going to zero as an inverse power of temperature, $\lambda_m \rightarrow T^{\frac{1-d}{2}}$.

3 Time dependent correlators

In this section, we present the main equations of our paper. We begin with the general expression for the time ordered thermal correlator, from which all subsequent results can be derived. We then specialize to the retarded Green's function. The central quantity of interest is the time-ordered correlator of two gauge-singlet operators. In the vector model it reads

$$\begin{aligned} G(t, \mathbf{y}) &\equiv \frac{2^{d+2} \pi^d}{\Gamma^2(\frac{d-2}{2})} \frac{1}{N} \langle \text{Tr} |\Phi^2(t, \mathbf{y})| \text{Tr} |\Phi^2(0)| \rangle \\ &= \sum_{j=1}^N \left(\sum_{m=-\infty}^{\infty} \frac{e^{im\lambda_j}}{(\cos(t + i\beta m) - \cos \theta)^{\frac{d-2}{2}}} \right)^2 \\ &= \int_{-\pi}^{\pi} d\lambda \rho(\lambda) \left(\sum_{m=-\infty}^{\infty} \frac{e^{im\lambda}}{(\cos(t + i\beta m) - \cos \theta)^{\frac{d-2}{2}}} \right)^2, \end{aligned} \quad (3.1)$$

where we have introduced a multiplicative constant on the first line that cancels the constant numerical factor that arises from the Wick contractions of the scalars. This has no effect on the physics but streamlines all subsequent equations. The explicit factor of $1/N$ guarantees that the two-point correlation function does not scale with N .

The corresponding expression in the adjoint model is

$$\begin{aligned} G(t, \mathbf{y}) &\equiv \frac{2^{d+2} \pi^d}{\Gamma^2(\frac{d-2}{2})} \frac{1}{N^2} \langle \text{Tr} |\Phi^2(t, \mathbf{y})| \text{Tr} |\Phi^2(0)| \rangle \\ &= \int_{-\pi}^{\pi} d\lambda d\lambda' \rho(\lambda) \rho(\lambda') \left(\sum_{m=-\infty}^{\infty} \frac{e^{im(\lambda-\lambda')}}{(\cos(t + i\beta m) - \cos \theta)^{\frac{d-2}{2}}} \right)^2. \end{aligned} \quad (3.2)$$

The final equality in either equation holds in the continuum limit $N \rightarrow \infty$ and the dependence of Eq. (3.2) on the difference of eigenvalues is a manifestation of the unbroken center symmetry of the underlying gauge theory [14]. We observe that the correlation function in the adjoint theory can be obtained from the one in the vector theory by simply replacing λ by $\lambda - \lambda'$ in (3.1) and including an additional integral¹ over λ' . As a consequence, we will mainly show

¹Note that by explicitly limiting the support of the eigenvalue distribution to $(-\pi, \pi]$ and extending the domain of integration to the whole real line, we can alternatively express Eq. (3.2) as

$$\int_{-\infty}^{\infty} d\lambda (\rho \star \rho)(\lambda) \left(\sum_{m=-\infty}^{\infty} \frac{e^{im\lambda}}{(\cos(t + i\beta m) - \cos \theta)^{\frac{d-2}{2}}} \right)^2.$$

Adjoint model results are then obtained by replacing the eigenvalue distribution $\rho(\lambda)$ by the convolution $\rho \star \rho$.

derivations for the vector model in the following, and only display final results for the adjoint theory.

The above expressions for time dependent correlators are most readily obtained through analytic continuation of the equal time correlators of [9],

$$G(\mathbf{y}) = \sum_j \left(\sum_m \frac{e^{im\lambda_j}}{(\cosh m\beta - \cos \theta)^\sigma} \right)^2 \quad (3.3)$$

by sending $\beta m \rightarrow \beta m - it$. The denominator follows from the corresponding expression for the vacuum two point correlator of the same singlet operators. The nontrivial new ingredient here compared to the vacuum result is the dependence on the eigenvalues of the $U(N)$ matrix that implements the singlet constraint. For completeness, we include a derivation from first principles in Appendix B.² Note that we have effectively implemented a thermal normal ordering procedure that subtracts the square of the one-point function from the correlation functions. In a different language, we have redefined the field operators such that their one-point function vanishes.

In what follows, we will also be using the retarded correlator of singlet operators, defined as

$$G_R(x, t) \equiv \frac{2^{d+2}\pi^d}{\Gamma^2(\frac{d-2}{2})} \frac{1}{N} \Theta(t) \text{Im} \langle \text{Tr}|\Phi^2(x, t)|\text{Tr}|\Phi^2(0)| \rangle. \quad (3.4)$$

In order to extract it from Eq. (3.1), it is useful to rewrite the sum over n inside the integral over eigenvalues,

$$G(t, \mathbf{x}) = \int_{-\pi}^{\pi} d\lambda \rho(\lambda) \left(\frac{1}{(\cos t - \cos \theta)^{\frac{d-2}{2}}} + 2 \sum_{m=1}^{\infty} \text{Re} \left[\frac{e^{im\lambda}}{(\cos(t + i\beta m) - \cos \theta)^{\frac{d-2}{2}}} \right] \right)^2. \quad (3.5)$$

Since the thermal sums are manifestly real and non-singular, any imaginary contribution must necessarily involve the vacuum piece. Consequently, we have

$$G_R(x, t) = \Theta(t) \left\{ \text{Im} \left[\frac{1}{(\cos t - \cos \theta)^{d-2}} \right] + 4 \text{Im} \left[\frac{1}{(\cos t - \cos \theta)^{\frac{d-2}{2}}} \int_{-\pi}^{\pi} d\lambda \rho(\lambda) \sum_{m=1}^{\infty} \text{Re} \left[\frac{e^{im\lambda}}{(\cos(t + i\beta m) - \cos \theta)^{\frac{d-2}{2}}} \right] \right] \right\}. \quad (3.6)$$

The first term is the well-known vacuum contribution to the retarded propagator. It is insensitive to the singlet constraint and has support only on the boundary light cone. The second term is a thermal contribution that depends on the eigenvalue distribution. We will discuss it in more detail in section 5.3.2. In Fourier space, the retarded correlator contains information about the spectrum of the theory, which has important implications for the dual bulk physics. We discuss this next.

²Following [9], one can perform the integral over λ to obtain an expression in terms of Fourier cosine coefficients of the eigenvalue distribution. Since we will not make much use of that representation in the present work, we refrain from showing it here.

4 Evanescent modes

Wave propagation in an AdS black hole background in standard gravity theory includes so called evanescent modes with an exponential fall-off towards the boundary whose existence is tied to the event horizon in the bulk spacetime geometry [16]. Finding such modes in an exotic theory with massless higher spin fields is a strong indication of the presence of black hole-like structures in that theory. In this section we demonstrate that the retarded propagator at high temperatures in our free singlet models indeed has precisely the right form to support evanescent modes in a dual bulk interpretation.

In thermal field theory, the spectral density is defined as the imaginary part of the retarded propagator in frequency-momentum space. In the low energy phase of singlet theories, it is expected to only receive contributions from $\omega^2 \geq \mathbf{k}^2$. This follows from the interpretation of the low temperature phase in terms of a thermal gas of higher spin particles. In the bulk, it receives only on-shell contributions and since the square of the momentum in the direction normal to the boundary is positive definite, one has $\omega^2 = \mathbf{k}^2 + k_z^2 \geq \mathbf{k}^2$.

A nontrivial geometric structure in the bulk can, however, support modes for which k_z is complex. In this case the mode amplitude is exponentially suppressed radially towards the boundary or, conversely, exponentially growing in the radial direction into the bulk interior. Such a mode can nevertheless remain normalizable if the bulk geometry is such that the exponential growth is cut off at some radial position. This happens for instance in the presence of a horizon in the bulk where modes with complex k_z propagate parallel to the horizon but are exponentially suppressed towards the boundary and thus effectively confined to the near horizon region. In the corresponding boundary theory the signature of a bulk evanescent mode is an exponentially suppressed but non-vanishing spectral density in the far off-shell regime $\omega \ll T \ll |\mathbf{k}|$. Such contributions were discovered previously in a planar limit of a free gauge singlet model [13]. The planar limit corresponds to the infinite temperature limit in our conventions. Using our approach, it is straightforward to look for evanescent mode signatures at finite temperature and we indeed find that they persist at high temperatures of both the adjoint and vector models. More specifically, we see that the presence of evanescent modes is directly linked to having a nontrivial eigenvalue distribution in the dual gauge theory.

As always in the free boundary theories that we are considering, the bulk interpretation of the results involves a degree of extrapolation. The above picture of evanescent modes propagating in the near horizon region of a black hole relies on having a classical bulk geometry and thus an effective field theory on the gravitational side of the duality. On the other hand, a spectral density of the above form is a robust signal that one can look for in any field theory. Accordingly, we can take evanescent behaviour in the boundary spectral function as one of the defining features of a bulk black hole away from the limit where we have an effective field theory description on the bulk side of the duality.

Note that since we are ultimately interested in large momenta $k \equiv |\mathbf{k}| \gg 1$, we can use a flat Fourier space representation of the correlation function. This simplifies the calculation considerably but it should be kept in mind that the description breaks down for small

momenta.

In principle, the spectral density in the evanescent regime could be obtained from a direct Fourier transformation of Eq. (3.6) in the flat limit. We find it convenient, however, to take an extra step and first obtain the retarded correlator in mixed k - t -space. To this end we use the relation $G_R(k, t) = \Theta(t) \text{Im} G(k, t)$, which remains valid in momentum space as the transformation from position space does not introduce a complex phase. The time ordered correlator in k - t space can be written as

$$G(k, t) = \int d\lambda \rho(\lambda) \int d^{d-1}p_1 d^{d-1}p_2 \delta^{(d-1)}(\mathbf{k} - \mathbf{p}_1 - \mathbf{p}_2) G_T(p_1, t, \lambda) G_T(p_2, t, \lambda) \quad (4.1)$$

with

$$G_T(p, t, \lambda) = \frac{1}{2p} \left[e^{-ipt} \left(\Theta(t) + n_B(p - i\frac{\lambda}{\beta}) \right) + e^{ipt} \left(\Theta(-t) + n_B(p + i\frac{\lambda}{\beta}) \right) \right]. \quad (4.2)$$

This essentially corresponds to Eq. (B.6), derived in Appendix B. In comparison, we have here performed the contraction on the eigenvectors of the gauge holonomy, used that $E \approx p$ in the high momentum limit, and replaced the sum over eigenvalues by its continuum approximation. The corresponding retarded correlator can be expressed as

$$G_R(k, \omega) = \int dt d^{d-1}p_1 d^{d-1}p_2 e^{i\omega t} \delta^{(d-1)}(\mathbf{k} - \mathbf{p}_1 - \mathbf{p}_2) G_R(p_1, p_2, t), \quad (4.3)$$

with

$$\begin{aligned} G_R(p_1, p_2, t) &= \Theta(t) \text{Im} \left[\int d\lambda \rho(\lambda) G_T(p_1, t, \lambda) G_T(p_2, t, \lambda) \right] \\ &= \frac{i\Theta(t)}{8p_1 p_2} \int d\lambda \rho(\lambda) \left[\left(1 + n(p_1 + i\frac{\lambda}{\beta}) + n(p_2 + i\frac{\lambda}{\beta}) \right) \left(e^{-it(p_1+p_2)} - e^{it(p_1+p_2)} \right) \right. \\ &\quad \left. + \left(n(p_1 + i\frac{\lambda}{\beta}) - n(p_2 + i\frac{\lambda}{\beta}) \right) \left(e^{it(p_1-p_2)} - e^{-it(p_1-p_2)} \right) \right]. \end{aligned} \quad (4.4)$$

We have used the fact that $\rho(\lambda)$ is even and that there are no purely thermal contributions to the retarded correlator in accordance with Eq. (3.6). Since $G_R(p_1, p_2, t)$ is manifestly real, taking the imaginary part of Eq. (4.3) allows us to drop the Θ -function. Integrating over t then yields a set of δ -functions and we immediately observe that those that depend on $p_1 + p_2$ will not contribute in the evanescent regime $\omega \ll k$, due to the δ -function in Eq. (4.3). Setting them to zero and integrating over p_2 in the remaining terms yields

$$\begin{aligned} \text{Im} G_R(k, \omega) &= \int d\lambda \rho(\lambda) \int d^{d-1}p \frac{1}{8p|\mathbf{k} - \mathbf{p}|} \left(n(p + i\frac{\lambda}{\beta}) - n(|\mathbf{k} - \mathbf{p}| + i\frac{\lambda}{\beta}) \right) \\ &\quad \times (\delta(\omega + p - |\mathbf{k} - \mathbf{p}|) - \delta(\omega - p + |\mathbf{k} - \mathbf{p}|)). \end{aligned} \quad (4.5)$$

By virtue of the δ -functions, we can rewrite this as

$$\begin{aligned} \text{Im } G_R(k, \omega) = & \int d\lambda \rho(\lambda) \int d^{d-1}p \frac{1}{16p} \\ & \left[\frac{1}{p+\omega} \left(n(p+i\frac{\lambda}{\beta}) - n(p+\omega+i\frac{\lambda}{\beta}) \right) \delta(\omega+p-|\mathbf{k}-\mathbf{p}|) \right. \\ & \left. - \frac{1}{p-\omega} \left(n(p+i\frac{\lambda}{\beta}) - n(p-\omega+i\frac{\lambda}{\beta}) \right) \delta(\omega-p+|\mathbf{k}-\mathbf{p}|) \right]. \end{aligned} \quad (4.6)$$

Working to lowest order in ω in the evanescent regime, this can in turn be approximated by

$$\text{Im } G_R(k, \omega) = -\omega \int d\lambda \rho(\lambda) \int d^{d-1}p \frac{1}{8p^2} n'(p+i\frac{\lambda}{\beta}) \delta(p-|\mathbf{k}-\mathbf{p}|). \quad (4.7)$$

The above expression only has support for $p \gg \beta$. There, the Bose distribution becomes a Boltzmann distribution, allowing us to integrate over λ to obtain

$$\text{Im } G_R(k, \omega) = \frac{\beta\omega\rho_1}{4k} \frac{\pi^{\frac{d-2}{2}}}{\Gamma(\frac{d-2}{2})} \int dp p^{d-4} d\theta \sin^{d-4} \theta e^{-\beta p} \delta(\theta - \arccos \frac{k}{2p}). \quad (4.8)$$

Here, we have assumed a symmetric eigenvalue distribution and introduced its first Fourier cosine moment, $\rho_1 \equiv \int d\lambda \rho(\lambda) \cos \lambda$, non-vanishing only for a non-constant eigenvalue distribution. The limits for the integration over p have to be adjusted such that the δ -function can be satisfied. In the evanescent regime, the limits are $k/2$ and ∞ . Integrating over both θ and p then yields

$$\begin{aligned} \text{Im } G_R(k, \omega) & \approx \frac{\pi\omega\rho_1}{4} \left(\frac{\pi k}{\beta} \right)^{\frac{d-5}{2}} K_{\frac{d-3}{2}} \left(\frac{k\beta}{2} \right) \\ & \approx \frac{\pi\omega\rho_1}{4k} \left(\frac{\pi k}{\beta} \right)^{\frac{d-4}{2}} e^{-\frac{k\beta}{2}}. \end{aligned} \quad (4.9)$$

with the modified Bessel function $K_\alpha(x)$. Evanescent behavior signaled by the exponential is thus seen above the phase transition, for both adjoint and vector models in any number of dimensions $d \geq 3$. In fact, for vector models the evanescent modes actually appear already below the phase transition (at temperatures scaling as T_c with N). This is a direct consequence of the phase transition being third order and the Fourier cosine mode ρ_1 changing continuously at T_c . Similar effects are observed for example in the free energy [10].

We find it remarkable that our simple boundary theories give rise to black hole-like behavior in the dual higher spin gravity or tensionless string theory. We note that the coefficient $\beta/2$ in the exponent that we find in free singlet theories differs from the corresponding coefficient obtained in supergravity [17]. While there is no *a priori* reason for the exponents in supergravity and higher spin gravity to agree, it would be interesting to understand the relation between the two.

5 General behavior of two-point correlation functions

In this section we study the time dependence of the correlation function Eq. (3.1) at general temperatures with an eye towards a bulk interpretation. In particular, we will observe exponentially decaying correlation functions in the high temperature phase, a well-known signature of bulk black holes in holographic CFTs [18]. Another important result of this section is the emergence of a previously unnoticed characteristic time scale at high temperature, beyond which the time dependence of the two-point correlation function resembles that of its low temperature counterpart. We observed a corresponding length scale in our earlier study of equal time correlation functions [9].

To simplify the analysis, we mainly focus on the so-called autocorrelator, where the operators are inserted at coincident spatial points, leaving only a dependence on their time difference. The discussion is divided into a few subsections. First, we develop a more transparent representation of the correlation function that holds at coincident spatial points. We then develop analytic approximations valid at very low and very high temperatures respectively. In particular, we contrast ubiquitous power law tails at low temperatures with exponential decay in even boundary dimensions in the high temperature phase. Following this, we present a numerical study of the correlation function at intermediate temperatures. Among other things, we uncover a new characteristic time scale in the numerical data that appears at high temperature and signals the return to a power law decay with time of the autocorrelator.

5.1 Coincident points

As before, the derivation we present is for the vector model and only results are quoted for adjoint representation scalars. To get started, we use basic trigonometric identities (taking the principal value of the square root for odd d) to rewrite Eq. (3.1) for $\theta = 0$ as

$$G(t) = (-2)^{2-d} \int d\lambda \rho(\lambda) \left(\sum_{m=-\infty}^{\infty} \frac{e^{im\lambda} (\text{sgn}(m))^d}{\sin^{d-2} \left(\frac{t+i\beta m}{2} \right)} \right)^2, \quad (5.1)$$

where we have assumed $t > 0$ for simplicity. Eq. (5.1) takes form of an integral over a square of a Fourier sum. The discontinuity of the function inside the sum, when viewed as a function of m , leads to complications in odd boundary dimensions that hamper a derivation of a simpler expression for arbitrary temperatures. As a result, our results for odd dimensions explicitly will rely on an approximate evaluation of Eq. (5.1). In even dimensions, on the other hand, the function is continuous and we can express it as a sum over images using the Poisson summation formula,

$$G(t) = (-2)^{2-d} \int d\lambda \rho(\lambda) \left(\sum_{k=-\infty}^{\infty} h_t^{(d)}(\lambda + 2\pi k) \right)^2, \quad (5.2)$$

where we have defined

$$h_t^{(d)}(\lambda) \equiv \int_{-\infty}^{\infty} dm e^{im\lambda} \frac{1}{\sin^{d-2} \left(\frac{t+i\beta m}{2} \right)} \quad (5.3)$$

as the Fourier transform of the function inside the summation. The higher dimensional $h_t^{(d)}(\lambda)$ can be obtained from the $d = 4$ expression as follows

$$h_t^{(d)}(\lambda) = \frac{2^{d-4}}{(d-3)!} \left[\prod_{n=1}^{\frac{d-4}{2}} (n^2 + \partial_t^2) \right] h_t^{(4)}(\lambda), \quad (5.4)$$

so it suffices to calculate the Fourier transform only for $d = 4$. We obtain

$$h_t^{(4)}(\lambda) = -\frac{4\pi}{\beta} \operatorname{csch} \left(\frac{\pi\lambda}{\beta} \right) \partial_t e^{\frac{(\pi-t)\lambda}{\beta}}, \quad (5.5)$$

which readily follows from expressing $h_t^{(4)}(\lambda)$ in terms of an incomplete Euler beta function, $B_x(a, b) \equiv \int_0^x s^{a-1}(1-s)^{b-1} ds$ and using the reflection identity

$$B_z(a, b) = (-z)^{-a} z^a \left(\left(\frac{1}{z} \right)^{a+b} (-z)^{a+b} B_{\frac{1}{z}}(1-a-b, b) + B(a, 1-a-b) \right). \quad (5.6)$$

The above expression for the autocorrelator is not amenable to analytic arguments for general temperatures but it can be evaluated numerically to good precision, as we shall see later on in this section. Before presenting our numerical results, however, we want to take advantage of certain simplifications that occur at high temperature to obtain analytic results that reveal properties of the high-temperature phase of the model. We have to evaluate the sum

$$\sum_{k=-\infty}^{\infty} e^{-\frac{(\lambda+2\pi k)t}{\beta}} \left(1 + \coth \left(\frac{\pi(\lambda+2\pi k)}{\beta} \right) \right). \quad (5.7)$$

In the regime $\beta \ll 1$, we can to leading order set the hyperbolic cotangent to $\operatorname{sgn}(k)$ unless $k = 0$. This limit holds for $-\pi < \lambda < \pi$, and since Eq. (5.7) is periodic, the approximation can be periodically extended beyond the original region of validity. Contributions for $k < 0$ can then be neglected and we obtain for the sum

$$e^{-\frac{\lambda t}{\beta}} \left(1 + \coth \left(\frac{\pi\lambda}{\beta} \right) + 2 \sum_{k=1}^{\infty} e^{-\frac{2\pi k t}{\beta}} \right) = e^{-\frac{\lambda t}{\beta}} \left(\coth \left(\frac{\pi t}{\beta} \right) + \coth \left(\frac{\pi\lambda}{\beta} \right) \right), \quad (5.8)$$

and for the correlator Eq. (5.2) in even dimensions for $\beta \ll 1$

$$G(t) = \frac{2^{d-2}\pi^2}{((d-3)!)^2} \frac{1}{\beta^2} \int d\lambda \rho(\lambda) \left[\left(\prod_{n=1}^{\frac{d-4}{2}} (n^2 + \partial_t^2) \right) \partial_t \left(e^{-\frac{\lambda t}{\beta}} \left(\coth \left(\frac{\pi t}{\beta} \right) + \coth \left(\frac{\pi\lambda}{\beta} \right) \right) \right) \right]^2. \quad (5.9)$$

For adjoint scalars, Eq. (5.2) is replaced by

$$G(t) = (-2)^{2-d} \int d\lambda d\lambda' \rho(\lambda) \rho(\lambda') \left(\sum_{k=-\infty}^{\infty} h_t(\lambda - \lambda' + 2\pi k) \right)^2, \quad (5.10)$$

and the even-dimensional high temperature correlator

$$G(t) = \frac{2^{d-2}\pi^2}{((d-3)!)^2} \frac{1}{\beta^2} \int d\lambda d\lambda' \rho(\lambda)\rho(\lambda') \times \left[\left(\prod_{n=1}^{\frac{d-4}{2}} (n^2 + \partial_t^2) \right) \partial_t \left(e^{-\frac{(\lambda-\lambda')t}{\beta}} \left(\coth\left(\frac{\pi t}{\beta}\right) + \coth\left(\frac{\pi(\lambda-\lambda')}{\beta}\right) \right) \right) \right]^2 \quad (5.11)$$

takes the place of Eq. (5.9).

5.2 Low temperatures: Power laws

At temperatures below the phase transition in the adjoint case and at $\beta \leq \mathcal{O}(1)$ in the vector model, the correlator is obtained from a constant $\rho(\lambda)$. The λ -integration in Eq. (5.1) then picks out the diagonal elements of the square and one obtains

$$G(t) = 2^{d-2} \sum_{m=-\infty}^{\infty} (\cosh(m\beta) - \cos t)^{2-d}. \quad (5.12)$$

For $t \ll \beta$, the vacuum piece, $m = 0$, dominates, implying a power law decay for small t ,

$$G(t) \sim \frac{1}{t^{2(d-2)}}. \quad (5.13)$$

At somewhat higher temperatures, such that there exist times that are much longer than the time that corresponds to the thermal wavelength, yet smaller than the AdS period, we can consider the leading order contribution in β . In the regime $\beta \ll t \ll 1$ we obtain

$$G(t) \approx 2^{d-1} \sum_{n=1}^{\infty} \frac{1}{(t^2 + \beta^2 n^2)^{d-2}} \approx \frac{2^{d-1}}{\Gamma(d-2)} \partial_t^{d-3} \left[\frac{1}{2t^2} \left(\frac{\pi t}{\beta} \coth\left(\frac{\pi t}{\beta}\right) - 1 \right) \right]. \quad (5.14)$$

In this regime the autocorrelator approaches another power law tail with an altered exponent

$$G(t) \sim \frac{1}{\beta t^{2d-5}}, \quad (5.15)$$

as could already have been anticipated on dimensional grounds. The behavior outlined in this subsection persists at all temperatures below the phase transition, $T < T_c$. We shall demonstrate this towards the end of section 6, after Eq. (6.8).

5.3 Ultra-high temperatures

We now consider very high temperatures under the assumption that the eigenvalue distribution can be well described by a δ -function.³ For simplicity, we first focus on insertions at the

³As explained in Section 6, for the vector model this is only valid for $d \geq 4$. However, even in the $d = 3$ case it proves instructive to compare to the δ -function limit, which is why we nevertheless include this case here.

same point in space, *i.e.* set $\theta = 0$, and then take θ to be non-vanishing but small. Moreover, we observe rather different behavior of correlation functions in even and odd boundary dimensions and thus find it useful to distinguish between the two.

5.3.1 Even dimensions: Exponential decay

In even boundary dimensions correlation functions exhibit a period of exponential decay in the high temperature phase, as expected if black hole-like objects were present in the bulk. We demonstrate this first by direct summation of Eq. (5.1) in the short time limit, where the expressions are particularly simple. We then establish the general results that follow from Eqs. (5.9) and (5.11).

For short times and $\rho(\lambda) = \delta(\lambda)$, we expand the summand in Eq. (5.1) in t and β ,

$$\begin{aligned} \sum_{m=-\infty}^{\infty} \frac{(\text{sgn}(m))^{d-2}}{\sin^{d-2}\left(\frac{t+i\beta m}{2}\right)} &\approx 2^{d-2} \sum_{m=-\infty}^{\infty} \frac{1}{(t+i\beta m)^{d-2}} \\ &\approx \frac{2^{d-2}\pi}{\beta} \frac{1}{(d-3)!} \frac{\partial^{d-3}}{\partial t^{d-3}} \coth\left(\frac{\pi t}{\beta}\right). \end{aligned} \quad (5.16)$$

For the time ordered correlator we then obtain

$$G(t) \approx \frac{2^{d-2}\pi^2}{\beta^2} \left[\frac{1}{(d-3)!} \frac{\partial^{d-3}}{\partial t^{d-3}} \coth\left(\frac{\pi t}{\beta}\right) \right]^2. \quad (5.17)$$

For instance, in $d = 4$, we have

$$G(t) \approx \frac{4\pi^4}{\beta^4} \text{csch}^4\left(\frac{\pi t}{\beta}\right). \quad (5.18)$$

As opposed to the expression below the transition (see Eqs. (5.13) and (5.15) above), no power law tails are present. At sufficiently late times, $t \gtrsim \beta$, we thus observe an exponentially decaying correlation function in even dimensions.

For arbitrary times, we insert $\rho(\lambda) = \delta(\lambda)$ directly into Eqs. (5.9) and (5.11) for the vector and adjoint models, respectively. In both cases we obtain

$$G(t) = \frac{2^{d-2}}{((d-3)!)^2} \frac{1}{\beta^2} \left[\left(\prod_{n=1}^{\frac{d-4}{2}} (n^2 + \partial_t^2) \right) \left(1 + \frac{\pi^2}{\beta} \text{csch}^2\left(\frac{\pi t}{\beta}\right) \right) \right]^2. \quad (5.19)$$

Compared to Eq. (5.17), we observe additional contributions that are a consequence of considering the theory on a sphere. In particular, we always find a constant contribution to the correlators. The exponential decay thus comes to a halt once the t -dependent part becomes of the same order as this constant piece, at $t \sim \log T/T$. After that the correlator remains approximately constant for a while.

We emphasize that this behavior persists for smeared operators. In fact, we can obtain all the above results for general θ . Focusing on the simpler example of small times, small θ

yields

$$\begin{aligned}
G(t, \theta) &\approx \frac{2^{d-2}}{\Gamma^2(\frac{d-2}{2})} \left[\partial_{\theta^2}^{\frac{d-4}{2}} \sum_{n=-\infty}^{\infty} \frac{1}{(\beta n - it)^2 + \theta^2} \right]^2 \\
&\approx \frac{2^{d-4} \pi^2}{\Gamma^2(\frac{d-2}{2}) \beta^2} \left[\partial_{\theta^2}^{\frac{d-4}{2}} \frac{\coth(\frac{\pi(t+\theta)}{\beta}) - \coth(\frac{\pi(t-\theta)}{\beta})}{\theta} \right]^2. \tag{5.20}
\end{aligned}$$

Expanding the above for $\theta \ll t$ reveals an exponential decay in time for all angles that are well localized inside the light cone. Accordingly, smearing the fields does not affect decay properties of the correlation functions in even dimensions. Let us highlight that the exponential decay is a direct consequence of the high temperature phase. We have demonstrated it in the limit of ultrahigh temperatures, and will confirm it at intermediate temperatures $T \gtrsim T_c$ in our numerical analysis in section 5.4, as well as analytically in section 6.

5.3.2 Odd dimensions: Retarded Green's functions supported inside the light cone

As mentioned earlier, away from the light cone, the retarded propagator Eq. (3.6) receives contributions only from the thermal piece, and only in odd dimensions. There, it reads

$$\begin{aligned}
G_R(x, t)|_{\cos t \neq \cos \theta} &= 4(-1)^{\frac{d-3}{2}} \Theta(t) \Theta(\cos \theta - \cos t) |\cos t - \cos \theta|^{-\frac{d-2}{2}} \\
&\quad \times \int_{-\pi}^{\pi} d\lambda \rho(\lambda) \sum_{m=1}^{\infty} \text{Re} \left[\frac{e^{im\lambda}}{(\cos(t + i\beta m) - \cos \theta)^{\frac{d-2}{2}}} \right] \tag{5.21}
\end{aligned}$$

for the vector model, while the result in the adjoint model is obtained by inserting the corresponding convolution. As we can see, its nontrivial nature within the light cone is directly linked to a non-constant eigenvalue distribution. In Appendix D we check how absence of light cone interior support in even boundary dimensions is consistent with the expected support inside the light cone for odd dimensional bulk wave equations.

In the limit of coincident spatial points, we can extract the analytical form of the time-ordered correlator from the $\lambda \rightarrow 0$ limit of Eq. (5.1), by using well known properties of the Polygamma functions that appear in an explicit summation. As anticipated, we will observe a non-vanishing imaginary part. For odd d , Eq. (5.1) becomes

$$\begin{aligned}
G(t) &= -2^{2-d} \left(\frac{1}{\sin^{d-2}(\frac{t}{2})} + 2i \sum_{m=1}^{\infty} \text{Im} \left[\frac{1}{\sin^{d-2}(\frac{t+i\beta m}{2})} \right] \right)^2 \\
&= -2^{2-d} \left[\frac{1}{\sin^{d-2}(\frac{t}{2})} + \frac{2^{d-2} i}{(d-3)!} \prod_{n=1}^{\frac{d-3}{2}} \left(\frac{(2n-1)^2}{4} + \partial_t^2 \right) \sum_{m=1}^{\infty} \text{Im} \left[\frac{1}{\sin(\frac{t+i\beta m}{2})} \right] \right]^2, \tag{5.22}
\end{aligned}$$

irrespective of the scalar representation. The last sum essentially corresponds to the definition of the Q -Polygamma function $\psi_q(z)$ and can be written as

$$\sum_{m=1}^{\infty} \text{Im} \left[\frac{1}{\sin\left(\frac{t+i\beta m}{2}\right)} \right] = \frac{2}{\beta} \text{Re} \left[\psi_{e^{-\frac{\beta}{2}}}\left(1 - i\frac{t}{\beta}\right) - \psi_{e^{-\frac{\beta}{2}}}\left(1 + i\frac{2\pi - t}{\beta}\right) \right]. \quad (5.23)$$

For $t > \beta$ the above can be approximated by

$$\frac{2}{\beta} \text{Re} \left[\psi_{e^{-\frac{\beta}{2}}}\left(1 - i\frac{t}{\beta}\right) - \psi_{e^{-\frac{\beta}{2}}}\left(1 + i\frac{2\pi - t}{\beta}\right) \right] \approx -\frac{4}{\beta} \log \cot \frac{t}{4}. \quad (5.24)$$

Consequently, one finds for $d = 3$

$$G(t) \approx -\frac{1}{2} \left[\frac{1}{\sin \frac{t}{2}} - \frac{4i}{\beta} \log \cot \frac{t}{4} \right]^2. \quad (5.25)$$

We note the dimensionally reduced form of the second term, dominant at $t \gg \beta$. It is logarithmic at small t , just as a massless correlator in $d = 2$, i.e. in one dimension less. This holds in any dimension, since the result in higher dimensions follows by simple differentiation. A small t expansion for $d > 3$ yields

$$G(t) \sim \frac{1}{\beta^2} \frac{1}{t^{2(d-3)}}. \quad (5.26)$$

This effective dimensional reduction is a well known feature of thermal quantum field theories. We note in particular the difference in exponent to Eq.(5.15), the late time behavior in the low temperature phase.

The retarded autocorrelator can be read off directly from Eq. (5.22). For our example of $d = 3$, one obtains

$$G_R(t) \approx -\frac{4}{\beta} \frac{\log \cot \frac{t}{4}}{\sin \frac{t}{2}}. \quad (5.27)$$

In summary, we observe a nontrivial imaginary part for the retarded correlator inside the light cone in odd boundary dimensions in the high temperature phase. Moreover, we have given an explicit expression for the time ordered Green's function at spatial coincidence, recognizing a dimensionally reduced form for $t \gg \beta$, when thermal effects are dominant.

5.4 Intermediate temperatures: Numerical results

In an intermediate regime, where the eigenvalue distribution can neither be approximated by a constant nor a δ -function, the correlation functions are best evaluated numerically. This allows us to single out effects of a nontrivial eigenvalue distribution, revealing shortcomings of the δ -function approximation discussed in Section 5.3 in low boundary dimensions. A new time scale t_a emerges in our plots. This is very similar to what we found in equal time correlators in [9]. The new scale is explained analytically in Section 6. Since the δ -function essentially cancels the λ integration that implements the singlet constraint, we refer to the

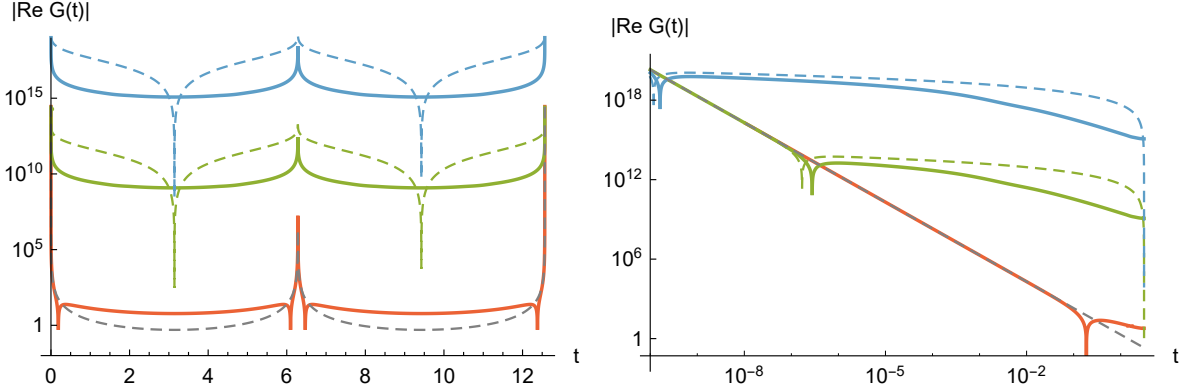


Figure 2. Vector model, $d=3$. $|G(t)|$ for $\beta/\beta_c = 50$ (red), $\beta/\beta_c = 10^{-3}$ (green) and $\beta/\beta_c = 10^{-6}$ (blue), with $t_a \sim 3 \cdot 10^{-3}$ in both high temperature cases. The gray dashed line depicts the vacuum correlator, while the colored dashed lines correspond to an unconstrained theory at the respective temperature, displayed only for $\beta < \beta_c$. The logarithmic plot on the left illustrates the periodicity of the correlators, as well as the renormalized low temperature behavior (shifted red curve) for $t > t_a$. More of the features can be extracted from the log-log plot on the right.

results of the δ -function approximation as the *unconstrained theory*. It is included in the plots for comparison.

At sufficiently low temperatures, a direct numerical summation of Eq. (5.1) is feasible. Good precision is obtained for an upper summation limit of the order of $10/\beta$. At high temperatures, instead, with $\beta \ll 1$, the expressions to be evaluated are different in odd and even boundary dimensions. In odd dimensions, we interpret Eq. (5.1) as a Riemann sum, thus effectively considering

$$G(t) = (-2)^{2-d} \int d\lambda \rho(\lambda) \left(\frac{1}{\sin^{d-2}(\frac{t}{2})} + 2i \operatorname{Im} \int_1^\infty dm \frac{e^{im\lambda}}{\sin^{d-2}(\frac{t+i\beta m}{2})} \right)^2, \quad (5.28)$$

or the adjoint model equivalent thereof. In even dimensions we instead work directly with Eqs. (5.9) and (5.11).

Key features of the correlation functions are displayed in the figures. In discussing their behavior, we distinguish the cases of even and odd dimensions. All plots were obtained for $N = 10^5$ and varying β . In Figs. 2 and 3 we show numerical solutions for both the vector and adjoint models for $d = 3$. This thus includes the canonical dimension for higher spin/CFT duality. We observe the following behavior:

$t \ll \beta$: At short times, the real part of the correlator is dominated by the power law decay of the vacuum contribution, included in all plots as a gray dashed line.

$t \sim \beta$: Characteristic zeros appear. Analogous zeros appear in Green's functions in Einstein gravity black holes in four bulk dimensions, and are associated with “ringing” behavior [19–21]. In our case, the number of zeros is small and the ringing thus rudimentary.

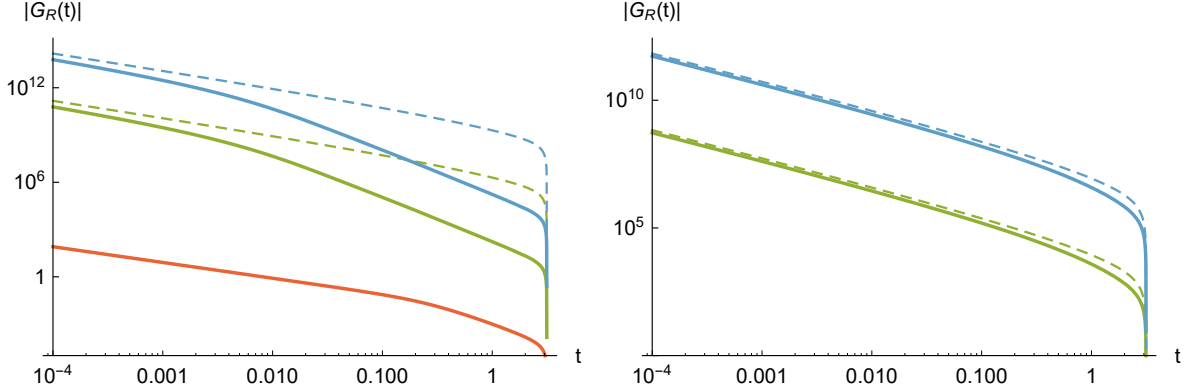


Figure 3. $d=3$, retarded correlator $G_R(t) = \text{Im } G(t)$. *Left:* Vector model for $\beta/\beta_c = 50$ (red), $\beta/\beta_c = 10^{-3}$ (green) and $\beta/\beta_c = 10^{-6}$ (blue). The dashed lines depict the result of an unconstrained theory at the corresponding temperatures. The crossover times are as in Fig. 2. *Right:* Adjoint model for same values of β/β_c . The imaginary part vanishes below the transition. The crossover times are at $t_a \sim 1$ for both lines.

$\beta \ll t \ll t_a$: The decay slows down significantly. For decreasing β/β_c , the correlator approaches that of an unconstrained theory and significantly departs from a thermal AdS boundary-boundary correlation function. We observe an effective dimensional reduction of the correlators, as pointed out towards the end of section 5.3.2.

$t \sim t_a$: At this time, the correlator exhibits a cross-over from the unconstrained behavior to a renormalized low temperature behavior, as evident in the left panel of Fig. 2. In $d = 3$, this effect prevents the zero-crossing for $t \rightarrow \pi$ found in the unconstrained theory. In higher dimensions, the crossover scale depends on β/β_c and for sufficiently small β/β_c increases beyond the radius of the sphere [9]. Also the retarded propagator $G_R(t) = \text{Im } G(t)$, displayed in Fig. 3, is sensitive to this scale. Beyond it, it decays significantly faster than its unconstrained counterpart.

As discussed at length in previous sections, the even dimensional correlators exhibit a characteristic exponential decay at times of the order of β . This can be clearly seen in Figure 4, both for fundamental and adjoint matter. In particular, the right hand side of the figure corresponds to the zero 't Hooft coupling limit of the well-known duality between strings on $AdS_5 \times S^5$ and $\mathcal{N} = 4$ SYM. We can summarize the behavior as follows:

$t \ll \beta$: At short times, the correlator is again dominated by the power law decay of the vacuum contribution, included in the plots as a gray dashed line.

$t \sim \beta$: At temperatures above the transition, correlations decay exponentially fast. The decay continues until finite volume and finite temperature effects become important.

$\beta \ll t \ll t_a$: The correlator approaches a constant value set by the temperature and by λ_m . For the vector model, we observe a significant discrepancy between the exact behavior

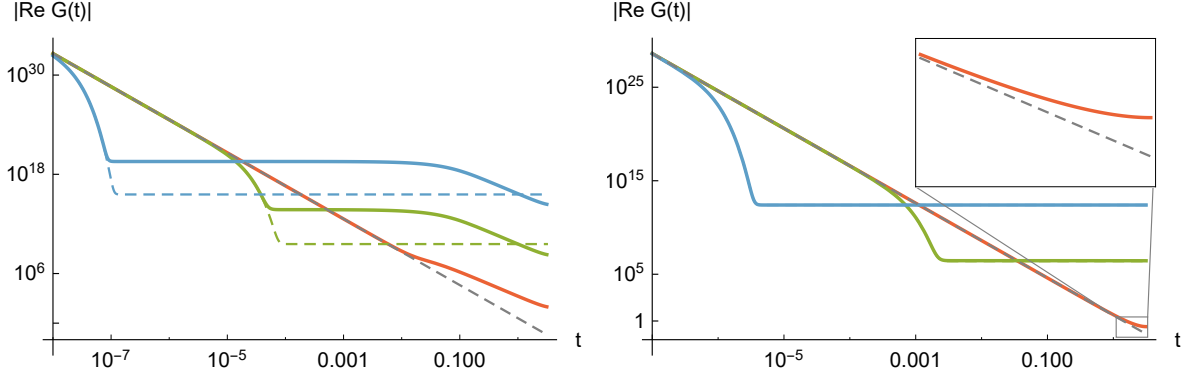


Figure 4. $d = 4$. *Left:* Vector model for $\beta/\beta_c = 10$ (red), $\beta/\beta_c = 10^{-3}$ (green) and $\beta/\beta_c = 10^{-6}$ (blue). The solid lines correspond to the exact behavior, while the dashed lines illustrate the unconstrained theory. The gray dashed line depicts the vacuum correlator. The crossover times in the high temperature phase are in order of increasing temperature $t_a \simeq 0.15$ and 0.18 . *Right:* Adjoint model for the same values of β/β_c . Line styles are as on the left. The crossover times are beyond the light crossing time of the sphere.

and the unconstrained theory, due to the finite width of the eigenvalue distribution, manifest in the ratio $\lambda_m/\beta \gtrsim 1$. These subtleties are discussed in Section 6.

$t \sim t_a$: Around this time the form of the correlations return to that of the low-temperature phase provided β/β_c is sufficiently close to 1 (such that $t_a < \pi$). For the temperatures we plot, $t_a \sim 10^{-1}$ for the vector model, while it is far greater than π in the adjoint model. Consequently, the adjoint correlators agree almost perfectly with the unconstrained behavior.

6 Finite volume effects in the high temperature phase

In some regimes, we can probe physics that is hard to understand from a picture of a simple uniform source at the center of an asymptotically thermal AdS space. From our previous observation of an emergent length scale in spatial correlators [9], one expects a corresponding time scale, t_a , beyond which the deviation of the eigenvalue distribution from a δ -function becomes visible. We have explicitly seen the emergence of such a time scale in our numerical data of the previous section. There is a relatively simple conceptual argument for this scale, which can be made more quantitative for certain parameter values. The new length and time scales are proportional to the radius of the $d - 1$ -sphere and therefore only visible at finite spatial volume.

In the expression (5.1) for the correlation function $G(t)$,

$$\int d\lambda \rho(\lambda) \left(\sum_{m=-\infty}^{\infty} \frac{e^{im\lambda}}{\left(\sin^2\left(\frac{t+i\beta m}{2}\right)\right)^{\frac{d-2}{2}}} \right)^2 = \int d\lambda \rho(\lambda) \left(\sum_{m=-\infty}^{\infty} \frac{e^{im\beta\frac{\lambda}{\beta}}}{\left(\sin^2\left(\frac{t+i\beta m}{2}\right)\right)^{\frac{d-2}{2}}} \right)^2, \quad (6.1)$$

the summation over m is a Fourier series representation of a function $f_t^{(d)}(\lambda/\beta)$. A δ -function limit of the eigenvalue distribution corresponds to expanding f_t in powers of λ , which can only yield a good approximation if $\lambda \ll \beta$ for all λ in the support of $\rho(\lambda)$. Thus, in the absence of extra conditions on t , $\lambda_m \ll \beta$ is required.

The consequences of the above inequality vary with dimension. From our expressions (2.6) for the asymptotic values for λ_m , we conclude that the requirement is violated at all temperatures for the vector model in $d = 3$. For the vector model in $d = 4$, it is fulfilled at temperatures that are exponentially large in N , while in higher even dimensions, it is easily satisfied high above the phase transition, measured on the scale of T_c . In the adjoint model on the other hand, the δ -function approximation works well already at temperatures only slightly above the transition. See Table 1 for a summary of the relevant temperature scales in different dimensions.

A more quantitative analysis can be carried out. Choosing for illustrative purposes $d = 4$, we consider the expression in real λ -space Eq. (5.9) (here for the vector model), slightly reformulated to read

$$G(t) = \frac{4\pi^2}{\beta^4} \int d\lambda \rho(\lambda) e^{-\frac{2\lambda t}{\beta}} \left[\lambda \left(\coth\left(\frac{\pi t}{\beta}\right) + \coth\left(\frac{\pi \lambda}{\beta}\right) \right) + \pi \operatorname{csch}^2\left(\frac{\pi t}{\beta}\right) \right]^2. \quad (6.2)$$

By expanding $\coth\left(\frac{\pi \lambda}{\beta}\right)$ in a series of exponentials, rewriting powers of λ as time derivatives of $e^{-\lambda t/\beta}$, and using $\rho(\lambda)|_{|\lambda|>\lambda_m} = 0$, we observe that all terms in the above expression are of the form

$$f(t) \partial_t^n \left(\int_0^\infty d\lambda \rho(\lambda) \left(e^{-\frac{2\lambda}{\beta}(t+\pi k)} \pm e^{-\frac{2\lambda}{\beta}(-t+\pi k)} \right) \right), \quad (6.3)$$

with different functions $f(t)$ and non-negative integers n and k . Recognizing the Laplace transform of ρ , denoted by $\bar{\rho}$, this corresponds to

$$f(t) \partial_t^n \left(\bar{\rho} \left(\frac{2(t+\pi k)}{\beta} \right) \pm \bar{\rho} \left(\frac{2(-t+\pi k)}{\beta} \right) \right). \quad (6.4)$$

The emergence of the additional time scale t_a is evident already at this stage, since $\bar{\rho}$ inevitably depends on the scale λ_m . We can make this statement more precise, however. At large temperatures, under the condition⁴ that $\lambda_m \gg \beta$, the leading contribution to $G(t)$ comes from those terms in (6.4) for which $k = 0$. There, an explicit integration of Eq. (6.2),

⁴This is precisely the case when the crossover time t_a is below the light crossing time of the sphere.

obtained by writing it as an integral over positive λ only and setting $\coth\left(\frac{\pi\lambda}{\beta}\right) = 1$, yields

$$G(t) \approx \frac{4\pi^4}{\beta^4} \sum_{n=0}^2 \pi^{-n} \binom{2}{n} \operatorname{csch}^{4-n}\left(\frac{\pi t}{\beta}\right) \left(e^{-\frac{n\pi t}{\beta}} \bar{\rho}^{(n)}\left(-\frac{2t}{\beta}\right) + (-1)^n e^{\frac{n\pi t}{\beta}} \bar{\rho}^{(n)}\left(\frac{2t}{\beta}\right) \right) \quad (6.5)$$

We can infer almost all essential details of the correlator from here, using the following generic features of the Laplace transform of the eigenvalue density:

- (i) $\bar{\rho}^{(n)}(x) \sim (-\lambda_m)^n$ for $|x| \ll \lambda_m^{-1}$,
- (ii) $\bar{\rho}(x) \rightarrow (\lambda_m x)^{-1} + \frac{e^{-x\lambda_m}}{x^2\lambda_m^2}$ for $|x| \gg \lambda_m^{-1}$.

These properties follow directly from the known behavior of the eigenvalue distribution in real λ -space. For $x \ll \lambda_m^{-1}$, their Laplace transforms follow that of a δ -function, with corrections parametrized by the only scale in the problem, λ_m . The large- x fall-off, on the other hand, follows from the fact that the distributions are approximately constant for sufficiently small λ . It is here that the deviation from a δ -function distribution becomes truly significant. The exponential contribution follows from the cut-off of $\rho(\lambda)$ at $\lambda = \lambda_m$. Note that the exponential growth for $x < 0$ will be overpowered by the exponentially decaying factors in Eq. (6.5), as we see below.

Using the above, we obtain the following behavior for the correlation function. At very short times, the vacuum contribution dominates, hidden in the $n = 0$ -term of the above sum. Once t becomes of order of β , there is a period of exponential decay, easily seen by inserting case (i) into Eq. (6.5). The dominant contributions are

$$G(t) \approx \frac{16\pi^2}{\beta^4} \left(4\pi^2 e^{-\frac{4\pi t}{\beta}} + 4\pi\lambda_m e^{-\frac{2\pi t}{\beta}} + \lambda_m^2 \right). \quad (6.6)$$

As we see, the exponential decay is eventually stopped by the constant term, at $t \sim \log \lambda_m/T \sim \log(T/T_c)/T$ for $T > T_c$, where there is a gap in the eigenvalue density. This constant in turn decays once the central part of the eigenvalue distribution becomes accessible, at $t/\beta \sim \lambda_m^{-1}$ or equivalently $t \sim t_a$ with

$$t_a \equiv \frac{\beta}{\lambda_m}. \quad (6.7)$$

We obtain the late time behavior by inserting case (ii) into Eq. (6.5). All exponential pieces are negligible, in particular since $t > t_a \gg \beta$ and $\lambda_m \leq \pi$. The only remaining contribution gives

$$G(t) \approx \frac{4\pi^2}{t^3\beta\lambda_m}. \quad (6.8)$$

Comparison with Eq. (5.15) for $d = 4$ shows the same decay as for the low temperature correlator, with a temperature dependent renormalization factor. We have thus analytically reproduced all features of Fig. 4.

As promised earlier, Eq. (6.5) also holds the key to seeing that the low temperature behavior of two successive power law regimes, as described in section 5.2, holds up until the

	$d = 3$	$d = 4$	$d \geq 5$
T_c	$N^{\frac{1}{2}}$	$N^{\frac{1}{3}}$	$N^{\frac{1}{d-1}}$
t_a	$N^{-\frac{1}{2}}$	$N^{-\frac{1}{3}} \log^{1/3} \left(\frac{T}{T_c} \right)$	$N^{-\frac{1}{d-1}} \left(\frac{T}{T_c} \right)^{\frac{d-4}{3}}$
T_a	—	$N^{\frac{1}{3}} e^N$	$N^{\frac{1}{d-4}}$

Table 1. Scaling of the critical temperature T_c , crossover time t_a and the constraining temperature T_a in the vector model for dimensions $d \geq 3$. The critical temperature follows directly from Eq. (2.5), while T_a is obtained from the condition $t_a \sim 1$, inserting the asymptotic expressions for λ_m , Eq. (2.6) in Eq. (6.7).

phase transition. The low temperature phase is characterized by the absence of the small parameter λ_m and the Laplace transform of ρ is always described by $\bar{\rho}(x) \sim x^{-1}$. This implies that the $n = 2$ term in Eq. (6.5) always dominates the thermal contributions, since derivatives of $\bar{\rho}$ are not suppressed. There is thus no leading exponential decay and the late time fall-off is given by the power law that is encoded in the Laplace transform, according to Eq. (6.8). Conversely, the argument confirms that the appearance of a dominant exponential regime is directly linked to the eigenvalue distribution becoming zero on a finite interval.

Similar arguments as above can be made for $d = 3$, although they are somewhat less clear due to the lack of description of the correlator in terms of elementary functions. A proof of concept goes as follows. For small β , the correlator is approximately described by Eq. (5.28), which after integration reads

$$G(t) = -\frac{1}{2} \int d\lambda \rho(\lambda) \left(\frac{1}{\sin\left(\frac{t}{2}\right)} - \frac{2i}{\beta} e^{-\frac{t\lambda}{\beta}} \operatorname{Re} B_{eit} \left(\frac{1}{2} + \frac{i\lambda}{\beta}, 0 \right) \right)^2. \quad (6.9)$$

For $t \ll 1$, the dominant contribution to the above comes from the $\lambda \rightarrow 0$ limit of the Beta function, since the latter can be expanded in a power series in λ , which converges quickly for $t \ll 1$. Higher powers of λ are then suppressed by powers of λ_m in the integrated expression. Moreover, there are cancellations which suppress the contributions from the integration over negative λ . In the small t limit we obtain

$$\begin{aligned} G(t) &\approx -2 \int d\lambda \rho(\lambda) \left(\frac{1}{t} + \frac{2i}{\beta} e^{-\frac{t\lambda}{\beta}} \log\left(\frac{t}{4}\right) \right)^2 \\ &\approx -2 \left(\frac{1}{t^2} + \frac{4i}{t\beta} \log\left(\frac{t}{4}\right) \bar{\rho}\left(\frac{t}{\beta}\right) - \frac{4}{\beta^2} \log^2\left(\frac{t}{4}\right) \bar{\rho}\left(2\frac{t}{\beta}\right) \right). \end{aligned} \quad (6.10)$$

We thus see that the logarithmic decay is accelerated once $t \gtrsim t_a$, in agreement with Figs. 2 and 3.

To summarize, the emergence of an additional time scale follows in the same way as an additional length scale in [9] from the fact that the integrand in all expressions for the correlator is a function of λ/β , and may be Taylor expanded in λ for general t only if $\lambda_m/\beta = t_a^{-1} \ll 1$.

We have moreover demonstrated analytically that the correlators become sensitive to the core of the eigenvalue distribution at times $t > t_a$. This leaves visible imprints on the eigenvalue distributions if t_a is smaller than the light crossing time of the sphere. The temperature dependence of λ_m implies that for $d > 3$, there is only a finite range of temperatures, $T_c \leq T \leq T_a$, in which this is true. We summarize the dependence of T_c and T_a on N and on d for the vector model in Table 1.

We see a manifestation of the scale t_a for a parametrically large window of temperatures which extends over all $T \geq T_c$ in $d = 3$, to exponentially high temperatures in $d = 4$ and to temperatures that grow like a positive power of N in $d \geq 5$. For adjoint scalars, on the other hand, since $T_c = \mathcal{O}(1)$, $T_a \simeq T_c$ for all d .

7 Discussion

In this section we summarize our findings, discuss connections to other developments and indicate some directions for future work. A concrete goal of our work is to assess the status of black holes in higher spin bulk theories that are in effect defined by the free gauge theories considered here. All our calculations have been carried out on the field theory side of the gauge/gravity duality and we work in the limit of vanishing 't Hooft coupling where the bulk interpretation of results is not *a priori* clear. We adopt an operational strategy and look for signatures in boundary correlation functions that are known, from previous studies at large 't Hooft coupling, to correspond to specific bulk features, e.g. black holes. In other words, if a bulk object looks like a black hole from the boundary perspective we call it black hole-like.

We work at finite temperature and finite volume throughout and all our results are obtained in a large N limit, where the physics can be analyzed in terms of saddle point solutions for the density of eigenvalues $\rho(\lambda)$ of the gauge holonomy around the thermal circle. The eigenvalue density determines the large N phase diagram of the theory and also governs the behavior of correlation functions of gauge invariant operators. The critical temperature for phase transitions on the unit $d-1$ -sphere is $T_c \sim 1$ for a singlet model with scalar matter in the adjoint representation and $T_c \sim N^{1/(d-1)}$ for a model with vector representation matter. In terms of bulk physics these critical temperatures correspond to $T_c \sim R_{AdS}^{-1}$ and $T_c \sim m_{Pl}$, respectively.

We have found evidence for black hole-like behavior previously observed in gauge/gravity duality in the limit where the bulk side of the duality is well described by classical gravity. It is useful to spell out a large N temperature ladder for discussing these results.

Low temperature: $T < T_c$ in adjoint model, $T \leq O(1)$ in vector model. Uniform eigenvalue density $\rho(\lambda) = \frac{1}{2\pi}$ in both models.

Super-AdS temperature: $1 \ll T \leq O(T_c)$ in vector model. The eigenvalue density is no longer uniform but no gap has opened up. This range is absent in the adjoint model where $T_c \sim 1$.

High temperature: $T_c < T$ in both vector and adjoint models. The eigenvalue density has developed a finite gap where $\rho(\lambda) = 0$.

Ultra-high temperature: $T_c < T_a \ll T$ in both types of models, where T_a is given in Table 1. It is defined to ensure that the eigenvalue density at higher temperatures is well approximated by a Dirac delta function (not strictly attainable in $d = 3$).

Our main results can be summarized as follows in relation to these temperature scales:

- We find evidence for evanescent modes (section 4) of the type pointed out in [16]. Evanescent behavior occurs in any $d \geq 3$ at super-AdS, high and ultra-high temperatures in the vector model and at all temperatures above the critical temperature in the adjoint model.
- We see a period of exponential decay in time of correlators (section 5.3.1) of the type pointed out in [18] for two boundary dimensions. We demonstrate this behavior explicitly for any even d at all temperatures above the phase transition in both vector and adjoint models. It is also visible in our numerical results for $t \lesssim \log(T/T_c)/T$ provided $T > T_c$.

The exponential decay is not immediately visible and it does not continue indefinitely. At very early times, short compared to the inverse temperature, the two-point correlation function decays according to a power law governed by the underlying scale symmetry of the model. Exponential decay sets in at $t \sim \beta$ and the correlation function settles to a constant value at $t \sim (\log T)/T$, which is maintained for a while. Eventually the periodicity of free wave propagation on the sphere sets in and the correlator returns to its initial value at $t = 2\pi$ in our units (see Figure 2).

We note that in even d , evanescent modes are evident at lower temperature than exponential time decay in vector models but appear together with exponential time decay at the critical temperature in adjoint models. In odd d we still see evanescent behavior but exponential decay in time is absent. Instead, we find what may be a new signal of black hole behavior in odd boundary dimensions:

- The boundary Green's function has support inside the light cone⁵ in odd d (section 5.3.2). This occurs at super-AdS, high, and ultra-high temperatures in vector models and at $T > T_c$ in adjoint models.

Finally, we have found a new time scale at which the time-dependence of boundary correlation functions changes qualitatively. This behavior is only detectable at high temperatures and finite volume, *i.e.* away from the planar limit in the bulk:

- For times beyond a new time scale t_a , boundary correlators return to their short-time, thermal AdS form, up to a temperature dependent normalization factor (see section 6,

⁵As opposed to only on the light cone.

especially Table 1). This behavior is seen at all high temperatures in $d = 3$, but only over a finite range of temperatures, $T_c < T < T_a$, in $d \geq 4$.

In the $d = 3$ vector model, we find the time scale $t_a = T_c^{-1} \sim N^{-1/2}$, and more generally, t_a is given in Table 1.

By the usual AdS/CFT dictionary, long boundary distances or late times translate to bulk features that are far removed from the boundary. Accordingly, we expect long-time correlators to probe more deeply into the bulk, while short-time correlators are mostly sensitive to propagation close to the boundary. Thus, very short $t \ll \beta$ only sense asymptotic AdS propagation, intermediate times $\beta \ll t \ll t_a$ can disclose the presence of black hole-like objects, while later times $t \gg t_a$ probe deep bulk features which are not accessible in a planar geometry.

Earlier studies (*e.g.* [10]) have cautiously refrained from interpreting the vector model phase transition as a sign of black holes in higher spin gravity. Our findings crucially add spatial extent to the picture. Our previous work [9] revealed a boundary spatial scale where equal time correlation functions at high temperature begin to depart from thermal AdS behavior, and we have now also confirmed a corresponding time scale consistent with bulk objects that grow with temperature. Since this boundary scale only comes into play at high temperature $T > T_c \sim m_{Pl}$, the corresponding black hole-like objects in the bulk have a minimum size, which scales with N in the same way as the Planck mass. Thus, the objects appear to become larger with increasing temperature and with decreasing gravitational coupling. The enormous size of these higher spin black hole-like objects demystifies their Planck scale temperature. They are analogous to standard large AdS black holes in Einstein gravity, whose Hawking temperature grows without bound with increasing black hole size. For a large enough AdS black hole, the Hawking temperature becomes trans-Planckian but this is not problematic as this is not the temperature measured by observers in free fall in the bulk spacetime geometry [22, 23]. Similar considerations presumably apply to very large higher spin black holes.

In free singlet theories, periods of exponential decay of correlations of approximately local field operators find their origin in an intricate cancellation of phases. In case of a two-dimensional boundary, infinite dimensional conformal symmetry on the cylinder dictates [27, 28] that thermal correlation functions in free boundary theories exhibit similar exponential fall-off behavior as their strongly interacting counterparts [18], even though they do not thermalize in the usual sense. On the torus, corresponding to finite size, the argument indicates exponentially decaying terms in the high temperature limit. Such arguments are not applicable in higher dimensions, and there is no a priori reason for an exponential fall-off. Moreover, delocalized Fourier space operators exhibit power law tails ([11] and Appendix C), much like the low temperature autocorrelators we discussed in section 5.2. The fact that thermal Green's functions of quasi-local operators nevertheless display periods of exponential decay may be taken as a sign that bulk higher spin theories retain features of their gravitational ancestors. In a sense, nontrivial phase cancellations are the only way for a free boundary theory to produce behavior similar to a strongly coupled CFT with a gravitational

dual.

Since our models are explicitly unitary and propagation in classical black hole backgrounds is known to break unitarity, our results must deviate from classical black hole results in a way that restores unitarity. In even dimensions we indeed found a cross-over from exponential decay to a constant correlator at a time $t \sim \log T/T$ valid above the phase transition. Qualitatively, the crossover is reminiscent of the results in [18] where an exponential decay crosses over to a non-decaying regime at late time, explained by the contribution from an alternative bulk manifold filling the same boundary. The sharpness of the transition visible in Fig. 4 suggests such an interpretation, but in the present higher spin case, we have no supporting bulk calculation. In vector models there is a later time t_a when the singlet constraint comes into operation and the correlation function develops another power law fall-off. This time the power law exponent is the same as in the low-temperature phase, but the correlation function picks up a temperature dependent normalization factor. In odd dimensions, a case not detailed in [18], we see a related crossover between two different power laws. We note that at high temperature this crossover coincides with a zero of the real part of the correlator (see Fig. 2).

In two boundary dimensions the advanced machinery of $d = 2$ conformal field theory has been applied to the tricky problem of reconciling the unitarity of CFT with the known, but approximate information loss in bulk black hole physics [24–26, 29]. We have glimpsed related behavior in higher dimensions for very particular models. It would be interesting to study these issues in more general high-dimensional models and look for similar effects.

The intriguing return to thermal AdS-like correlation functions after a period of black hole-like correlator behavior also deserves further study. We have observed this in the high temperature phase both at late times and large angle in low dimensions, suggesting that we are probing deep into the bulk. We have established that the high temperature phase displays black hole-like features, like evanescent modes, and a closer study of deep probes might reveal the inner workings of emergent black holes in higher spin gravity.

Acknowledgments

This work was supported in part by the Swedish Research Council through the Oskar Klein Centre, under contract 621-2014-5838 and under contract 335-2014-7424, the Icelandic Research Fund grant 163422-052 and the University of Iceland Research Fund.

A Saddle point evaluation of path integrals and eigenvalue distributions

We wish to evaluate the Euclidean path integral of a $U(N)$ gauge theory on $S^{d-1} \times S^1$ with scalar matter fields in the adjoint or fundamental representation,

$$Z[\beta] = \int \mathcal{D}A_\mu \mathcal{D}\phi \mathcal{D}\phi^\dagger e^{-S[A_\mu, \phi, \phi^\dagger; \beta]}, \quad (\text{A.1})$$

in the limit of vanishing gauge coupling. For a detailed derivation, including gauge fixing and evaluating the corresponding Faddeev-Popov determinants, see *e.g.* [14]. We do not repeat the derivation here but merely outline the main steps in order to motivate the eigenvalue distributions that we work with in the rest of the paper.

On a compact spatial manifold gauge invariance imposes the vanishing of all gauge charges and the only physical states are gauge singlets. In the free theory limit the gauge field decouples from the matter fields apart from a zero mode,

$$\alpha = \frac{1}{\text{Vol}(S^{d-1})} \int_{S^{d-1}} A_t, \quad (\text{A.2})$$

that enters into gauge covariant derivatives, $D_t = \partial_t + i\alpha$ in the vector model and $D_t = \partial_t + i[\alpha, \cdot]$ for an adjoint scalar [14]. The zero mode also gives rise to a gauge holonomy, $U = e^{i\beta\alpha}$, going around the thermal circle. The path integral over the gauge field reduces to a $U(N)$ matrix integral over the zero mode, which in turn reduces to an integral over the eigenvalues $e^{i\lambda_i}$ of the gauge holonomy matrix,

$$Z[\beta] = \frac{1}{N!} \int \left(\prod_i d\lambda_i \right) \exp \left[\sum_{i \neq j} \ln \left| \sin \left(\frac{\lambda_i - \lambda_j}{2} \right) \right| - \sum_i S_s[\lambda_i] \right]. \quad (\text{A.3})$$

The matter contribution to the action $S_s[\lambda]$ comes from integrating out the scalar field in the path integral (A.1), keeping track of the gauge field zero mode in the covariant derivative. In the vector model it is given by

$$S_s[\lambda_i] = -2N_f \sum_{k=1}^{\infty} \frac{1}{k} z_S^d(x^k) \cos(k\lambda_i), \quad (\text{A.4})$$

and in the adjoint model by

$$S_s[\lambda_i] = - \sum_{k=1}^{\infty} \frac{1}{k} z_S^d(x^k) \sum_j \cos(k(\lambda_i - \lambda_j)), \quad (\text{A.5})$$

where $z_S^d(x)$ is the scalar one-particle partition sum on a $d - 1$ -dimensional sphere,

$$z_S^d(x) = x^{\frac{d}{2}-1} \frac{1+x}{(1-x)^{d-1}}, \quad (\text{A.6})$$

with $x = e^{-\beta}$.

In the large N limit the integral over eigenvalues can be evaluated in a saddle point approximation. For this it is convenient to work with the eigenvalue distribution $\rho(\lambda) = \frac{1}{N} \sum_{i=1}^N \delta(\lambda - \lambda_i)$ or equivalently its Fourier cosine coefficients,

$$\rho_k = \int_{-\pi}^{\pi} d\lambda \rho(\lambda) \cos k\lambda = \frac{1}{N} \sum_{i=1}^N \cos k\lambda_i. \quad (\text{A.7})$$

In the large N limit the eigenvalue density approaches a continuum. It is positive semi-definite,

$$\rho(\lambda) \geq 0, \quad (\text{A.8})$$

and normalized to one in our conventions,

$$\int_{-\pi}^{\pi} d\lambda \rho(\lambda) = 1. \quad (\text{A.9})$$

By using the relation

$$\ln \left| \sin \left(\frac{\lambda_i - \lambda_j}{2} \right) \right| = -\log 2 - \sum_{k=1}^{\infty} \frac{1}{k} \cos(k(\lambda_i - \lambda_j)), \quad (\text{A.10})$$

and assuming that the eigenvalue distribution is symmetric under sign reversal $\lambda \rightarrow -\lambda$, the integrand in (A.3) can be re-expressed in terms of an effective action involving the eigenvalue distribution.⁶

In the vector model one finds

$$S = N^2 \sum_{k=1}^{\infty} \frac{\rho_k}{k} \left(\rho_k - 2 \frac{N_f}{N} z_S^d(x^k) \right). \quad (\text{A.11})$$

which is minimized by

$$\rho_k = \frac{N_f}{N} z_S^d(x^k). \quad (\text{A.12})$$

The corresponding eigenvalue density, given by

$$\rho(\lambda) = \frac{1}{2\pi} + \frac{N_f}{N} \sum_{k=1}^{\infty} z_S^d(x^k) \frac{1}{\pi} \cos(k\lambda), \quad (\text{A.13})$$

appears in equation (2.1) in the main text. The constant term in the eigenvalue density is needed for the normalization condition (A.9). As discussed in Section 2, the positivity condition (A.8) is satisfied for all $\lambda \in [-\pi, \pi]$ at low temperatures but there is a phase transition and in the high temperature phase the eigenvalue distribution develops a gap, *i.e.* there is a finite range $\lambda_m \leq |\lambda| \leq \pi$ where $\rho(\lambda) = 0$. The critical temperature (2.5) is determined by the condition $\rho(\pm\pi) = 0$.

At high T , but still below T_c , the eigenvalue density can be expressed in terms of a polylogarithm [9],

$$\rho(\lambda) = \frac{1}{2\pi} + A_d \left(\frac{T}{T_c} \right)^{d-1} \text{Re} \left(\text{Li}_{d-1}(e^{i\lambda}) \right), \quad (\text{A.14})$$

⁶Assuming a symmetric eigenvalue distribution leads to the apparent breaking of the \mathbb{Z}_n center symmetry of the adjoint model. The symmetry can be restored by summing over \mathbb{Z}_n images of the saddle point but this only leads to an overall factor and does not affect our results. In the vector model the center symmetry is broken from the start by the matter sector.

where $A_d = \frac{1}{2\pi(1-2^{2-d})\zeta(d-1)}$. At high temperatures beyond the phase transition the eigenvalue density is still given by a polylogarithm but now it vanishes over a finite interval,

$$\rho(\lambda) = \begin{cases} A_d \left(\frac{T}{T_c}\right)^{d-1} (\operatorname{Re} \operatorname{Li}_{d-1}(e^{i\lambda}) - \operatorname{Re} \operatorname{Li}_{d-1}(e^{i\lambda_m})) & \text{for } |\lambda| \leq \lambda_m, \text{ and} \\ 0 & \text{otherwise.} \end{cases} \quad (\text{A.15})$$

The maximal eigenvalue λ_m is fixed by the normalisation condition, $\int_{-\lambda_m}^{\lambda_m} \rho(\lambda) d\lambda = 1$, which can be expressed as follows in terms of polylogarithms,

$$\operatorname{Im} \operatorname{Li}_d(e^{i\lambda_m}) - \lambda_m \operatorname{Re} \operatorname{Li}_{d-1}(e^{i\lambda_m}) = \frac{1}{2A_d} \left(\frac{T_c}{T}\right)^{d-1}. \quad (\text{A.16})$$

In the limit of very high temperature the eigenvalue distribution is narrowly peaked around the origin. One obtains the scaling behavior (2.6) for the width of the eigenvalue distribution at $T \gg T_c$, and the eigenvalue distribution itself can be approximated by

$$\rho(\lambda) = \frac{A_d}{2} \left(\frac{T}{T_c}\right)^{d-1} \begin{cases} \pi(\lambda_m - |\lambda|) & \text{for } d = 3, \\ \frac{1}{2} (\lambda_m^2(3 - 2 \log \lambda_m) - \lambda^2(3 - 2 \log |\lambda|)) & \text{for } d = 4, \\ \zeta(d-3)(\lambda_m^2 - \lambda^2) & \text{for } d \geq 5. \end{cases} \quad (\text{A.17})$$

In the adjoint model the effective action takes the form

$$S = N^2 \sum_{k=1}^{\infty} \frac{(1 - z_S^d(x^k))}{k} \rho_k^2. \quad (\text{A.18})$$

As long as $z_S^d(x^k) < 1$, the favored configuration is a homogeneous distribution $\rho(\lambda) = \frac{1}{2\pi}$, which has $\rho_k = 0$ for all $k \geq 1$. There is a critical temperature at which $z_S^d(x_c) = 1$ and the first non-trivial Fourier cosine mode of the eigenvalue distribution condenses. The precise value of the critical temperature depends on the number of spatial dimensions but $T_c \sim \mathcal{O}(1)$ for all d . As we go to higher temperatures, above the phase transition, the higher modes successively condense and the detailed implementation of the positivity constraint on $\rho(\lambda)$ becomes somewhat intricate. The approximate expression (2.7) for the eigenvalue density, developed in [14], simplifies the analysis considerably and is sufficient for our purposes in this paper. In particular, it allows one to infer the correct scaling behavior of the width of the eigenvalue distribution at high temperatures, $\lambda_m \rightarrow T^{\frac{1-d}{2}}$.

B Time dependent Green functions

In singlet models, the main subtlety in constructing time dependent correlators lies in the implementation of the constraint. In the formalism of Schwinger and Keldysh [30, 31], this is achieved through various insertions of δ -functions that project onto physical states. A careful treatment of the integration along the complex time contour then gives rise to a generating functional of time-dependent correlation functions that obey the singlet conditions.

The free singlet models considered in the present work offer a significant shortcut via straightforward analytic continuation of the Euclidean propagator to the real time domain. In the vector theory the Euclidean propagator takes the form [9],

$$G_{iM}^{AB}(n) = \sum_{j=1}^N \frac{\Psi_j^A(\Psi_j^B)^\dagger}{\beta^{-2}(2\pi n + \lambda_j)^2 + E_\ell^2}, \quad (\text{B.1})$$

in frequency/angular momentum space. Here, $E_\ell = (\ell + (d-2)/2)$ and Ψ_i is an eigenvector of the gauge holonomy matrix that belongs to the eigenvalue $e^{i\lambda_i}$. The eigenvectors are taken to be normalized,

$$\sum_{A=1}^N \Psi_i^A(\Psi_j^A)^\dagger = \delta_{ij}, \quad \sum_{i=1}^N \Psi_i^A(\Psi_i^B)^\dagger = \delta^{AB}. \quad (\text{B.2})$$

Analytic continuation, $\beta^{-2}(2\pi n + \lambda_i)^2 \rightarrow -(\omega + i\epsilon)^2$ yields a momentum space expression for the retarded propagator,

$$G_{R,IM}^{AB}(\omega) = \frac{\delta^{AB}}{-(\omega + i\epsilon)^2 + E_\ell^2}. \quad (\text{B.3})$$

Using well-known thermal field theory relations between the time ordered propagator, the retarded propagator, and its discontinuity in presence of an imaginary chemical potential,⁷

$$G_T^{AB} = -i G_R^{AB} - 2 \text{Im} G_R^{AC} \sum_{j=1}^N n_B \left(\omega + i \frac{\lambda_j}{\beta} \right) \Psi_j^C(\Psi_j^B)^\dagger, \quad (\text{B.4})$$

one obtains after some manipulations the following time ordered propagator,

$$G_{T,IM}^{AB}(\omega) = \frac{i}{\omega^2 - E_\ell^2 + i\epsilon} \delta^{AB} + 2\pi\delta(\omega^2 - E_\ell^2) \sum_{j=1}^N n_B \left(|\omega| + i \frac{\omega}{|\omega|} \frac{\lambda_j}{\beta} \right) \Psi_j^A(\Psi_j^B)^\dagger. \quad (\text{B.5})$$

The fact that the eigenvalues of the holonomy matrix appear as an imaginary chemical potential is a well known feature of thermal correlation functions in gauge theories and follows from the holonomy matrix being the Lagrange multiplier that implements the gauge singlet constraint [11]. Fourier transforming Eq. (B.5) in time yields the mixed space expression,

$$G_T^{AB}(t, E) = \frac{1}{i} \frac{1}{2E} \sum_{j=1}^N \Psi_A^j(\Psi_B^j)^\dagger \times \left[e^{-iEt} \left(\Theta(t) + n_B(E - i \frac{\lambda_j}{\beta}) \right) + e^{iEt} \left(\theta(-t) + n_B(E + i \frac{\lambda_j}{\beta}) \right) \right]. \quad (\text{B.6})$$

⁷A nice derivation can for instance be found in [32].

Finally, Eq. (B.6) can be transformed to yield the real space expression (using time translational and rotational invariance to set one of the insertion points to $x = 0$)

$$G_T^{AB}(t, \mathbf{y}) = \frac{1}{i} \sum_{l,M} \frac{1}{2E_l} Y_{l,M}(\mathbf{y}) Y_{l,M}(0) \sum_{j=1}^N \Psi_A^j(\Psi_B^j)^\dagger \times \left[e^{-iE_l t} \left(\Theta(t) + n_B(E_l - i\frac{\lambda_j}{\beta}) \right) + e^{iE_l t} \left(\theta(-t) + n_B(E_l + i\frac{\lambda_j}{\beta}) \right) \right]. \quad (\text{B.7})$$

We can evaluate this expression further by using the fact that $Y_{l,M}(0) \propto \delta_{M,0}$ and inserting the form of the spherical harmonics for $M = 0$. First taking $t > 0$ and writing the distribution functions as sums over exponentials

$$G_T^{AB}(t, \mathbf{y}) = \frac{\Gamma(\sigma)}{4\pi^{\sigma+1}i} \sum_l C_l^{(\sigma)}(\cos \theta) \sum_{j=1}^N \Psi_A^j(\Psi_B^j)^\dagger \times \left[e^{-it(l+\sigma)} \left(1 + \sum_{n=1}^{\infty} e^{-\beta n(l+\sigma) + in\lambda_j} \right) + e^{it(l+\sigma)} \left(\sum_{n=1}^{\infty} e^{-\beta n(l+\sigma) - in\lambda_j} \right) \right], \quad (\text{B.8})$$

we find

$$G_T^{AB}(t, \mathbf{y}) = \frac{\Gamma(\sigma)}{4\pi^{\sigma+1}i} \sum_{j=1}^N \Psi_A^j(\Psi_B^j)^\dagger \times \left[\frac{1}{(2 \cos t - 2 \cos \theta)^\sigma} + \sum_{n=1}^{\infty} \frac{e^{in\lambda_j}}{(2 \cos(t - i\beta n) - 2 \cos \theta)^\sigma} + \sum_{n=1}^{\infty} \frac{e^{-in\lambda_j}}{(2 \cos(t + i\beta n) - 2 \cos \theta)^\sigma} \right], \quad (\text{B.9})$$

by recognizing the generating functional for the Gegenbauer polynomials $C_l^{(\sigma)}$. The evaluation for $t < 0$ is similar. All in all we finally obtain

$$G_T^{AB}(t, \mathbf{y}) = \frac{\Gamma(\sigma)}{4\pi^{\sigma+1}i} \sum_{j=1}^N \Psi_A^j(\Psi_B^j)^\dagger \times \left[\frac{1}{(4 \sin^2(\theta/2) - 4 \sin^2(t/2))^\sigma} + \sum_{n \neq 0} \frac{e^{in\lambda_j}}{(2 \cos(t + i\beta n) - 2 \cos \theta)^\sigma} \right]. \quad (\text{B.10})$$

By subsequently considering the corresponding Wick contractions, we arrive at the following expression for a time-ordered singlet-singlet correlator:

$$G(t, \mathbf{y}) \equiv \frac{2^{d+2}\pi^d}{\Gamma^2(\frac{d-2}{2})} \frac{1}{N} \langle \text{Tr}|\Phi^2(t, \mathbf{y})| \text{Tr}|\Phi^2(0)| \rangle = \sum_{m,n=-\infty}^{\infty} \frac{\sum_{j=1}^N e^{i(m+n)\lambda_j}}{(\cos(t + i\beta m) - \cos \theta)^{\frac{d-2}{2}} (\cos(t + i\beta n) - \cos \theta)^{\frac{d-2}{2}}}. \quad (\text{B.11})$$

The numerical factor has been chosen as to simplify all following expressions, while the factor of $1/N$ guarantees that the two-point function does not scale with N .

C Fourier space

Correlators of glueball operators $\text{Tr}F^2$ in the free limit of $\mathcal{N} = 4$ SYM were investigated in [11] for a flat boundary in mixed k - t -space as well as in k - ω -space. To compare, we can take the planar limit of our expressions in $d = 4$ and consider the corresponding Fourier transforms. As we shall see, in the limit of a δ -function eigenvalue distribution, our expressions agree with those of [11] up to the different number of derivatives in the definition of the operators. In the second part of this appendix we use the resulting expressions to directly extract the evanescent modes of section 4.

C.1 Retarded propagator

In the planar limit, the retarded propagator Eq. (3.6) becomes

$$G_R(x, t) = 4\Theta(t) \left(\text{Im}(-t^2 + x^2)^{-2} + 2 \text{Im}(-t^2 + x^2)^{-1} \sum_{m=1}^{\infty} \rho_m \text{Re} [((\beta m - it)^2 + x^2)^{-1}] \right). \quad (\text{C.1})$$

After appropriately introducing ϵ -factors to circumvent the poles, this expression can straightforwardly be transformed to momentum space to read

$$G_R(k, t) = \int d^3x e^{i\mathbf{k}\mathbf{x}} G_R(x, t) = 4\Theta(t) \left(\frac{\cos kt}{2t} + 4 \frac{\sin kt}{k} \sum_{m=1}^{\infty} \frac{\rho_m}{4t^2 + m^2\beta^2} \right). \quad (\text{C.2})$$

In the low temperature phase, when $\rho(m) \approx \delta_{m0}$, only the vacuum contributes. Beyond the phase transition, on the other hand, when $\rho(m) \approx 1$, we can carry out the summation to obtain

$$G_R(k, t) = \frac{4\Theta(t)}{k} \left(\frac{kt \cos kt - \sin kt}{2t^2} + \frac{\pi \sin kt}{t\beta} \coth \left(\frac{2\pi t}{\beta} \right) \right). \quad (\text{C.3})$$

We can readily transform the above expression to frequency space. We find, up to an overall factor of 4 due to our normalization in accordance with [11],

$$G_R(k, \omega) = -2 + \frac{4\pi i}{k\beta} \log \left(\frac{\Gamma(-\frac{i\beta}{4\pi}(\omega - k))}{\Gamma(-\frac{i\beta}{4\pi}(\omega + k))} \right) - \left(\frac{2\pi i}{k\beta} - \frac{\omega}{k} \right) \log \frac{\omega + k}{\omega - k}. \quad (\text{C.4})$$

C.2 Evanescence

In principle, we can extract the evanescent behavior derived in section 4 directly from Eq. (C.4). However, to allow for a nontrivial eigenvalue distribution, we will instead use Eq. (C.2) as our starting point. Since by definition, $G_R(k, t)$ is real, the imaginary part of $G_R(k, \omega)$ corresponds to the Fourier sine transform of $G_R(k, t)$. At the same time, since the term inside the brackets in Eq. (C.2) is odd under reflection of t , the domain of integration for the sine transform can be extended to the whole t -domain. Consequently, the integral can be directly calculated by contour integration. Explicitly, we have

$$\text{Im} G_R(k, \omega) = 2 \int_{-\infty}^{\infty} \left(\frac{\cos kt}{2t} + 4 \frac{\sin kt}{k} \sum_{m=1}^{\infty} \frac{\rho_m}{4t^2 + m^2\beta^2} \right) \sin \omega t, \quad (\text{C.5})$$

and thus

$$\begin{aligned} \text{Im } G_R(k, \omega) &= \frac{\pi}{2} (\text{sgn}(k + \omega) - \text{sgn}(k - \omega)) \\ &\quad - \sum_{m=1}^{\infty} \frac{\pi \rho_m}{2km\beta} \left(\Theta(k + \omega) e^{-\frac{m\beta}{2}(k+\omega)} - \Theta(k - \omega) e^{-\frac{m\beta}{2}(k-\omega)} \right. \\ &\quad \left. + \Theta(-k - \omega) e^{-\frac{m\beta}{2}(-k-\omega)} - \Theta(\omega - k) e^{-\frac{m\beta}{2}(\omega-k)} \right). \end{aligned} \quad (\text{C.6})$$

In the evanescent regime, neither the vacuum term nor the two final terms in the above sum contribute. Moreover, the dominant contribution arises for $m = 1$, due to the Boltzmann factors. These considerations imply the final result

$$\text{Im } G_R(k, \omega) \approx \frac{\pi \rho_1}{2k\beta} \left(e^{-\frac{\beta}{2}(k-\omega)} - e^{-\frac{\beta}{2}(k+\omega)} \right) \approx \frac{\pi}{4} \frac{\omega \rho_1}{k} e^{-\frac{\beta}{2}k}, \quad (\text{C.7})$$

in agreement with Eq. (4.9) for $d = 4$.

D Consistency check on bulk and boundary retarded propagator support

We can check explicitly how a low temperature bulk propagator which does not vanish inside the light cone is consistent with a boundary correlator without support inside the light cone, as should be the case in even boundary/odd bulk dimension. The CFT operator that we are considering has scaling dimension $\Delta = d - 2$ for a d -dimensional boundary theory. In the dual bulk theory, it is this conformal dimension which determines the analytic properties of the bulk-bulk correlator. In particular, consider its explicit expression at $T = 0$ in global coordinates, reviewed for example in [33],

$$G_{\Delta}(\xi) = C_{\Delta} \xi^{\Delta} {}_2F_1 \left(\frac{\Delta}{2}, \frac{\Delta + 1}{2}, \Delta - \frac{d}{2} + 1, \xi^2 \right), \quad (\text{D.1})$$

where C_{Δ} is a normalization factor unimportant to our discussion, ${}_2F_1$ is a hypergeometric function and

$$\xi \equiv \frac{\cos \rho \cos \rho'}{\cos t - \sin \rho \sin \rho' \cos \theta}, \quad (\text{D.2})$$

with ρ labeling the radial direction in global coordinates, with the boundary being at $\rho = \pi/2$ and the center of AdS at $\rho = 0$.

For $\Delta = d - 2$, the hypergeometric function simplifies and the bulk expression takes on the form

$$G_{\Delta}(\xi) = C_{\Delta} \xi^{d-2} (1 - \xi^2)^{\frac{1-d}{2}}. \quad (\text{D.3})$$

Hence, it picks up an imaginary part for even boundary/odd bulk dimensions⁸ whenever $\xi > 1$. This imaginary part, however, is confined to the bulk interior, as follows directly from

⁸In particular, this reassuringly implies that for a four-dimensional bulk, where the scalar is conformally coupled, the imaginary part of the propagator is purely due to its singularities.

the boundary-boundary correlator, which we obtain as

$$G(t, \theta) = C_{\Delta}^{-1} \lim_{\rho \rightarrow \frac{\pi}{2}} \lim_{\rho' \rightarrow \frac{\pi}{2}} \cos^{-\Delta} \rho \cos^{-\Delta} \rho' G_{\Delta}(\xi) = \frac{1}{(\cos t - \cos \theta)^{\Delta}}, \quad (\text{D.4})$$

in agreement with Eqs. (3.1) and (3.2) at $T \rightarrow 0$. As long as the bulk is well described by thermal AdS-space, this behavior persists, as follows from a direct extrapolation of Eq. (D.1) to finite temperatures.

References

- [1] I. Klebanov and A. Polyakov, “AdS dual of the critical O(N) vector model,” *Phys.Lett.* **B550** (2002) 213–219, [arXiv:hep-th/0210114](#) [[hep-th](#)].
- [2] S. Giombi, S. Minwalla, S. Prakash, S. P. Trivedi, S. R. Wadia, and X. Yin, “Chern-Simons Theory with Vector Fermion Matter,” *Eur. Phys. J.* **C72** (2012) 2112, [arXiv:1110.4386](#) [[hep-th](#)].
- [3] O. Aharony, G. Gur-Ari, and R. Yacoby, “d=3 Bosonic Vector Models Coupled to Chern-Simons Gauge Theories,” *JHEP* **03** (2012) 037, [arXiv:1110.4382](#) [[hep-th](#)].
- [4] E. Fradkin and M. A. Vasiliev, “On the Gravitational Interaction of Massless Higher Spin Fields,” *Phys.Lett.* **B189** (1987) 89–95.
- [5] E. Fradkin and M. A. Vasiliev, “Cubic Interaction in Extended Theories of Massless Higher Spin Fields,” *Nucl.Phys.* **B291** (1987) 141.
- [6] B. Sundborg, “Stringy gravity, interacting tensionless strings and massless higher spins,” *Nucl. Phys. Proc. Suppl.* **102** (2001) 113–119, [arXiv:hep-th/0103247](#).
- [7] E. Witten, “Anti-de Sitter space, thermal phase transition, and confinement in gauge theories,” *Adv. Theor. Math. Phys.* **2** (1998) 505–532, [arXiv:hep-th/9803131](#) [[hep-th](#)].
- [8] B. Sundborg, “The Hagedorn Transition, Deconfinement and N=4 SYM Theory,” *Nucl. Phys.* **B573** (2000) 349–363, [arXiv:hep-th/9908001](#).
- [9] I. Amado, B. Sundborg, L. Thorlacius, and N. Wintergerst, “Probing emergent geometry through phase transitions in free vector and matrix models,” *JHEP* **02** (2017) 005, [arXiv:1612.03009](#) [[hep-th](#)].
- [10] S. H. Shenker and X. Yin, “Vector Models in the Singlet Sector at Finite Temperature,” [arXiv:1109.3519](#) [[hep-th](#)].
- [11] S. A. Hartnoll and S. P. Kumar, “AdS black holes and thermal Yang-Mills correlators,” *JHEP* **12** (2005) 036, [arXiv:hep-th/0508092](#) [[hep-th](#)].
- [12] A. Jevicki and K. Suzuki, “Thermofield Duality for Higher Spin Rindler Gravity,” in *JHEP* [10], p. 094, [arXiv:1508.07956](#) [[hep-th](#)].
- [13] A. Jevicki and J. Yoon, “Bulk from Bi-locals in Thermo Field CFT,” *JHEP* **02** (2016) 090, [arXiv:1503.08484](#) [[hep-th](#)].
- [14] O. Aharony, J. Marsano, S. Minwalla, K. Papadodimas, and M. Van Raamsdonk, “The Hagedorn - deconfinement phase transition in weakly coupled large N gauge theories,” *Adv.Theor.Math.Phys.* **8** (2004) 603–696, [arXiv:hep-th/0310285](#) [[hep-th](#)].

- [15] D. J. Gross and E. Witten, “Possible Third Order Phase Transition in the Large N Lattice Gauge Theory,” *Phys. Rev.* **D21** (1980) 446–453.
- [16] S.-J. Rey and V. Rosenhaus, “Scanning Tunneling Macroscopy, Black Holes, and AdS/CFT Bulk Locality,” *JHEP* **07** (2014) 050, [arXiv:1403.3943 \[hep-th\]](#).
- [17] D. T. Son and A. O. Starinets, “Minkowski space correlators in AdS / CFT correspondence: Recipe and applications,” *JHEP* **09** (2002) 042, [arXiv:hep-th/0205051 \[hep-th\]](#).
- [18] J. M. Maldacena, “Eternal black holes in anti-de Sitter,” *JHEP* **0304** (2003) 021, [arXiv:hep-th/0106112 \[hep-th\]](#).
- [19] J. S. F. Chan and R. B. Mann, “Scalar wave falloff in asymptotically anti-de Sitter backgrounds,” *Phys. Rev.* **D55** (1997) 7546–7562, [arXiv:gr-qc/9612026 \[gr-qc\]](#).
- [20] J. S. F. Chan and R. B. Mann, “Scalar wave falloff in topological black hole backgrounds,” *Phys. Rev.* **D59** (1999) 064025.
- [21] V. Cardoso and G. Khanna, “Black holes in anti-de Sitter spacetime: Quasinormal modes, tails, and flat spacetime,” *Phys. Rev.* **D91** no. 2, (2015) 024031, [arXiv:1501.00977 \[gr-qc\]](#).
- [22] S. Hemming and L. Thorlacius, “Thermodynamics of Large AdS Black Holes,” *JHEP* **11** (2007) 086, [arXiv:0709.3738 \[hep-th\]](#).
- [23] E. J. Brynjolfsson and L. Thorlacius, “Taking the Temperature of a Black Hole,” *JHEP* **09** (2008) 066, [arXiv:0805.1876 \[hep-th\]](#).
- [24] E. Dyer and G. Gur-Ari, “2D CFT Partition Functions at Late Times,” *JHEP* **08** (2017) 075, [arXiv:1611.04592 \[hep-th\]](#).
- [25] A. del Campo, J. Molina-Vilaplana, and J. Sonner, “Scrambling the spectral form factor: unitarity constraints and exact results,” *Phys. Rev.* **D95** no. 12, (2017) 126008, [arXiv:1702.04350 \[hep-th\]](#).
- [26] H. Chen, C. Hussong, J. Kaplan, and D. Li, “A Numerical Approach to Virasoro Blocks and the Information Paradox,” *JHEP* **09** (2017) 102, [arXiv:1703.09727 \[hep-th\]](#).
- [27] J. L. Cardy, “Conformal invariance and universality in finite-size scaling,” *J. Phys.* **A17** (1984) L385–L387.
- [28] D. Birmingham, I. Sachs, and S. N. Solodukhin, “Conformal field theory interpretation of black hole quasinormal modes,” *Phys. Rev. Lett.* **88** (2002) 151301, [arXiv:hep-th/0112055 \[hep-th\]](#).
- [29] A. L. Fitzpatrick, J. Kaplan, D. Li, and J. Wang, “On information loss in AdS₃/CFT₂,” *JHEP* **05** (2016) 109, [arXiv:1603.08925 \[hep-th\]](#).
- [30] J. S. Schwinger, “Brownian motion of a quantum oscillator,” *J. Math. Phys.* **2** (1961) 407–432.
- [31] L. V. Keldysh, “Diagram technique for nonequilibrium processes,” *Zh. Eksp. Teor. Fiz.* **47** (1964) 1515–1527. [Sov. Phys. JETP20,1018(1965)].
- [32] M. Laine and A. Vuorinen, “Basics of Thermal Field Theory,” *Lect. Notes Phys.* **925** (2016) pp.1–281, [arXiv:1701.01554 \[hep-ph\]](#).
- [33] H. Nastase, *Introduction to the ADS/CFT Correspondence*. Cambridge University Press, 2015.